New aspects of enzymes working in lignocellulose degradation

Hanžek, Marija

UNIVERSITY OF ZAGREB

FACULTY OF FOOD TECHNOLOGY AND BIOTECHNOLOGY

GRADUATE THESIS

Zagreb, November 2017.

Marija Hanžek

861/BPI

NEW ASPECTS OF ENZYMES WORKING IN LIGNOCELLULOSE DEGRADATION

Experiments for this Graduate thesis were done at the Institute of Food Technology, University of Natural Resources and Life Sciences, Vienna. The thesis was made under guidance of Priv.-Doz. Dr. Roland Ludwig and with the help of Dipl.-Ing. Erik Breslmayr.

I would like to use this opportunity to thank Priv.-Doz. Dr. Roland Ludwig for accepting my application and giving me the chance to learn from him and be a part of his amazing team. I would also like to thank Dipl. Ing. Erik Breslmayr for all the help and patience during experiments to support this thesis (Institute of Food Technology, University of Natural Resources and Life Sciences, Vienna).

Furthermore, a big thanks to prof.dr.sc. Božidar Šantek for his advice and supervision (Department of Biochemical Engineering, Faculty of Food Technology and Biotechnology, Zagreb).

I na kraju, želim se neizmjerno zahvaliti svojoj obitelji te dečku i prijateljima, za potpunu podršku, bodrenje i razumijevanje.

TEMELJNA DOKUMENTACIJSKA KARTICA

Diplomski rad

Sveučilište u Zagrebu
Prehrambeno-biotehnološki fakultet
Zavod za biokemijsko inženjerstvo
Laboratorij za biokemijsko inženjerstvo, industrijsku mikrobiologiju i tehnologiju slada i piva

Znanstveno područje: Biotehničke znanosti
Znanstveno polje: Biotehnologija

NOVI ASPEKTI ENZIMA KOJI SUDJELUJU U RAZGRADNJI LIGNOCELULOZE

Marija Hanžek 861/BPI

Sažetak: Zbog povećane globalne potražnje za energijom, fosilne izvore potrebno je zamijeniti obnovljivim izvorima energije (npr. biomasom). Otkriće LPMO (litičke polisaharid monooksigenaze) bilo je ključno za razumijevanje prirodne razgradnje biomase. Glavna prepreka u istraživanju LPMO je nedostatak jednostavnog protokola za istraživanje enzimske aktivnosti pomoću spektroskopije. Sukladno tome, cilj ovog rada bio je razviti i potvrditi protokol za utvrđivanje enzimske aktivnosti te istodobno okarakterizirati LPMO izoliranu iz plijesni *Neurospora crassa*. Dokazano je da je reduktant 2,6-DMP (2,6-dimetoksifenol), zajedno sa novootkrivenim kosupstratom H_2O_2, najbolja kromogenska komponenta sa visokim molarnim apsorpcijskim koeficijentom (24.8 $mM^{-1}cm^{-1}$) u vidljivom dijelu spektra (469 nm). Optimalna aktivnost LPMO je u neutralnom prema bazičnom pH području. Najniža koncentracija LPMO koja može biti izmjerena i koja se razlikuje od vrijednosti slijepe probe je ~0.0125 μM.

Ključne riječi: *LPMO, 2,6-dimetoksifenol, vodikov peroksid, analiza, spektrofotometrija*

Rad sadrži: 58 stranica, 27 slika, 9 tablica, 32 literaturna navoda, 2 priloga
Jezik izvornika: engleski

Rad je u tiskanom i elektroničkom obliku (pdf format) pohranjen u: Knjižnica Prehrambeno-biotehnološkog fakulteta, Kačićeva 23, Zagreb

Mentor na Prehrambeno - biotehnološkom fakultetu: *prof. dr. sc. Božidar Šantek*
Neposredni voditelj: *priv. doz. dr. Roland Ludwig*, University of Natural Resources and Life sciences, Vienna
Pomoć pri izradi: *dipl. ing. Erik Breslmayr*

Stručno povjerenstvo za ocjenu i obranu:
1. Prof. dr. sc. *Blaženka Kos*
2. Prof. dr. sc. *Božidar Šantek*
3. Priv. doz. dr. *Roland Ludwig*
4. Doc. dr. sc. *Andreja Leboš Pavunc* (zamjena)

Datum obrane: 08. prosinac 2017.

BASIC DOCUMENTATION CARD

Graduate Thesis

University of Zagreb
Faculty of Food Technology and Biotechnology
Department of Biochemical Engineering
Laboratory for Biochemical Engineering, Industrial Microbiology and Malting and Brewing Technology

Scientific area: Biotechnical Sciences
Scientific field: Biotechnology

NEW ASPECTS OF ENZYMES WORKING IN LIGNOCELLULOSE DEGRADATION

Marija Hanžek, 861/BPI

Abstract: Fossil fuels have to be replaced by renewable energies (e.g. biomass) due to increasing global demand for energy. The discovery of LPMOs (lytic polysaccharide monooxygenases) was a breakthrough in understanding of how nature degrades biomass. The main obstacle in LPMO research is the lack of an easy to use spectroscopic activity assay. Accordingly, the aim of this thesis was to develop and validate an activity assay and concomitantly characterize the LPMO from the fungi *Neurospora crassa*. 2,6-DMP (2,6-dimethoxyphenol) as reductant in addition with the new co-substrate H_2O_2 was proven to be the best chromogenic compound with a high extinction coefficient (24.8 $mM^{-1}cm^{-1}$) in the visible range (469 nm). The optimal LPMO activity was observed in the neutral to basic pH range. The lowest concentration of LPMO, which could be measured and distinguished from blank reactions, was ~0.0125 μM.

Keywords: *LPMO, 2,6-dimethoxyphenol, hydrogen peroxide, assay, spectrophotometry*

Thesis contain: 58 pages, 27 figures, 9 tables, 32 references, 2 supplements
Original in: English

Graduate Thesis in printed and electronic (pdf format) version deposited in: Library of the Faculty of Food Technology and Biotechnology, Kačićeva 23, Zagreb

Mentor at Faculty of Food Technology and Biotechnology: *Božidar Šantek, PhD, Full professor*
Principal investigator: *Roland Ludwig, PhD, Priv.-Doz.*, University of Natural Resources and Life Sciences, Vienna
Technical support and assistance: *Erik Breslmayr, Dipl. Ing.*

Rewievers:
1. *Blaženka Kos*, PhD, Full professor
2. *Božidar Šantek*, PhD, Full professor
3. *Roland Ludwig*, PhD, Priv.- Doz.
4. *Andreja Leboš Pavunc*, PhD, Assistant professor (substitute)
Thesis defended: 08 December 2017

Contents

1. INTRODUCTION

Increasing global demand for energy together with global warming and decreasing reserves makes it obvious that fossil fuels must be replaced by alternative sources such as renewable energies (Dimarogona et al., 2012). The largest and also the most promising source for the production of fuels is biomass. In the form of energy, it provides around 10% of the global energy supply. Bioethanol is the biofuel which is produced in the biggest volume with an annual production of 84 billion liters (2010) projected to reach 175 billion liters until this year (2017). Present bioethanol is mostly produced from starch and sugars which are also potential food sources. A lot of researches have been done in order to develop biofuels based on biomass such as algal biomass or lignocellulosic materials, which are not used as food. Biofuels developed from lignocellulosic biomass are second-generation biofuels and can be produced in two ways, with thermochemical or biochemical processes (Horn et al., 2012). Of main interest are biochemical processes with lignocellulosic biomass. The conversion of lignocellulosic biomass to ethanol consists of two processes: cellulose and hemicellulose have to be degraded into simple sugars (saccharification) and afterwards these sugars are converted to ethanol by microorganisms (Dimarogona et al., 2013). The most sustainable technology for saccharification is enzyme technology, but there are limiting factors like the disparity of the plant cell wall and the recalcitrance of the individual components (cellulose, hemicelluloses, lignin). Formerly it was thought that only hydrolytic enzymes have a part in the degradation of these components. This system consists of enzymes acting randomly in the polysaccharide chain and acting at chain ends (Horn et al., 2012). However, because of the crystallinity of polysaccharide chains, which are tightly packed and not accessible for hydrolases, this mechanism was reconsidered when lytic polysaccharide monooxygenases (LMPOs) were discovered. The discovery of LPMOs was a significant breakthrough in our understanding of how nature degrades recalcitrant biomass (Hemsworth et al., 2013; Hemsworth et al., 2015). LPMOs are copper-dependent monooxygenases which require molecular oxygen and an external electron donor to function properly. These enzymes enhance efficiency of cellulases by acting on the surface of the insoluble substrate (Dimarogona et al., 2013; Kittl et al., 2012). Because of very big importance of LPMOs in the future degradation of biomass, the aim of this thesis was to develop and validate an activity assay (pH and temperature effects, limit of detection) and concomitantly characterize the LPMO from the fungi *Neurospora crassa* (*Nc*LPMO9C, also known as *Nc*U02916).

2. THEORY

2.1. ENZYME ASSAYS

Enzyme assays are done for two reasons, to identify an enzyme and prove its presence or absence in given sample and to determine the amount of an enzyme in the assay. There are two different approaches for enzyme assays: qualitative, in which positive or negative result is satisfactory and quantitative approach, in which data should be as accurate as possible. Enzymes have the advantage that they can be identified by their catalyzed reaction, but the problem is that even the same assay performed under identical conditions may yield different results because enzyme activity depends on numerous factors and general understanding of distinct enzyme is required, which cannot be described in all details in the enzyme assay protocol. Nature and strength of ions, pH and temperature are the conditions that must be strictly monitored if assays want to be reliably compared. Because of the great diversity of enzymes, assay procedures are adjusted to the features of the individual enzyme. When determining enzyme assay, it has to be considered that enzyme reactions depend not only on conditions mentioned above, but also on the concentration of all assay components. It is also important to be aware that compounds not directly involved in the reaction can influence the results (interactions of hydrophobic substances or detergents with the protein surface, metal ions, etc.).

Although each enzyme has its own characteristics and properties, there are some general rules valid for all enzyme assays. The aim of every assay is to monitor the time-dependent conversion of substrate in the product and procedure must have the ability to identify it. Since product formation is directly connected with the disappearance of the substrate, its decreasing can be a measure of the reaction. In case of two or more substrates, it is enough to measure only one of them. The main problem in measuring is that every method is more or less susceptible to scattering. It can have different origins and some of them cannot be avoided (instability of the instruments or measurements in turbid solutions), but some of them can at least be reduced by careful handling (contaminations, dust, air bubbles, etc.). It is also very important that only the observed component shows the signal (e.g. absorption), so the reaction actually starts at zero and any change in signal refers to ongoing reaction.

The simplest way to monitor the reaction is appearance and disappearance of the coloured compound. Invisible UV range can also be observed with spectrophotometers, and since practically all the compounds show absorption in this area, this extends the observation

range remarkably. Spectrophotometers are easy to handle and have low sensibility against disturbances so they are used very often. On the other hand, if an enzymatic reaction cannot be observed this way, some other optical methods (e.g. fluorimetry) are used. Beside optical methods, electrochemical methods are also in use. The mentioned methods can perform continuous and discontinuous assays. Continuous assays are very important in detecting reaction velocity and for evaluating the enzyme activity. They also enable detection of incorrect influence and the control of the reaction course (progress curve). Catalyzed reactions initially show a linear correlation, however, the substrate consumption slows down and finally breaks off the reaction. Therefore it is very important to determine enzyme velocity from the linear part of the curve. In order to determine velocity for a discontinuous (stopped) assay, reactions must be stopped after some time and the sample has to be analyzed with a separation method like HPLC. These methods provide only one single point and velocity is calculated from the slope of a line connecting that point and the blank (Bisswanger, 2014).

2.1.1. Dependence on substrates

Beside the enzyme, substrates and cofactors are the main components of the enzyme assay. Their purity, stability and state are crucial and therefore the highest demands have to be made. Usually, enzymes have a defined substrate according to their physiological function, however, many enzymes show wide specificity. A synthetic one can replace physiological substrate. In order to determine efficiency of the substrate, K_M and V_{max} values are calculated. The lower the $K_{M,}$ the better is the affinity to the substrate. It is not always the case to take the most efficient substrate, because availability, stability, solubility and the accessibility to a detection method have to be considered. The conclusion is that a physiological substrate is not always used, because to compare results it is more important to use the same substrate in all assays (Bisswanger, 2014).

2.1.2. Buffers and ions

Assays have to be done in buffers due to their role in adjustment and stabilization of the desired pH value. They consist of a weak acid and strong basic component. Not only pH range is important when choosing the buffer, but also its ionic strength, concentration and the

nature of its components. The more concentrated buffer system, the higher is the ability to stabilize the desired pH. However, the best concentration range is from 0.05 to 0.2 M. Ions affect enzyme activity both by their nature and ionic strength. The activity of an enzyme can differ if observed in two different buffer systems, even though they have the same pH and concentration. The capacity range of buffer is narrow, so if a broader pH range is required, several buffer systems can be combined (Bisswanger, 2014).

2.1.2.1. Solvents

Because of the cellular environment, water is the standard solvent for enzyme assays. However, for some enzymes, organic solvents have to be used in order to ensure that an essential component, which is not soluble in water, is also dissolved (Bisswanger, 2014).

2.1.3. Influence of pH

pH in the assay mixture can have big influence in enzyme activity. Most enzymes follow a bell-shaped curve, showing zero activity in the strong acid region, followed by increase up to the maximum value and decrease to zero in the strong alkaline region. This is the consequence of two effects, the native, three-dimensional protein structure of an enzyme and the state of protonation of the functional groups of amino acids and cofactors involved in the reactions. The maximum of the bell-shaped curve shows the highest activity of an enzyme and pH detected at this value is the pH optimum, which is usually chosen as the standard pH used in the assay of the distinct enzyme. The pH optimum of many enzymes is within the physiological range, ~7.5 (Bisswanger, 2014).

2.1.4. Influence of temperature

The curve showing correlation between temperature and enzyme activity is also bell-shaped as in previous case, increasing with rising temperature, reaching the maximum and decreasing afterwards. The maximum is also referred to temperature optimum, however, that temperature does not necessarily exist for all enzymes. The velocity of any chemical reaction

increases with the temperature, ~2-3 times every 10°C. On the other hand, 3D structure of enzymes is thermo-sensitive and high temperature can lead to denaturation, which is responsible for decrease of the activity. Therefore, for enzymes that have not been investigated yet, it should be ensured that the assay temperature is within the stability range. That temperature is determined by plotting activity versus different temperatures. After Arrhenius plot is made, the lower temperature range should be a straight line, indicating the area of stable enzyme. Because of denaturation, a straight line should show deviations in higher temperature range. One of three favoured temperatures is usually chosen, 25, 30 or 37°C (Bisswanger, 2014).

2.1.5. Limit of Detection (LoD)

One of the very important conditions is that substrate and product differ in observed characteristics. The product may be very well detected with the chosen method, but if the substrate shows a similar signal, no turnover can be observed. Often both substrate and product show a small difference in signal which is hard to quantify because the small signal becomes lost within the noise. As a rule, intensity of the reaction signal must be one or two factors higher than the noise. This is the reason why the limit of detection is determined (Bisswanger, 2014).

If an analyte (enzyme) is present, the produced signal should be high enough to reliably be distinguished from the analytical noise (signal produced in the absence of analyte). LoD is the lowest analyte concentration that can be reliably emphasized from the LoB. LoD is determined by using both the measured LoB and samples known to contain a low concentration of analyte. $LoD = LoB + 1.645(SD_{\text{low concentration sample}})$. Assuming a Gaussian distribution of the low concentration samples, 95% of values will go beyond the previously defined LoB, and only 5% of low concentration samples will go below the LoB and incorrectly appear to contain no analyte. A typical approach to estimate LoD consists of measuring replicates, usually ~20, of a blank sample, determining the mean value and standard deviation (SD), and calculating LoD as the mean +2x SD. The mean +3, 4 or even 10x SD can also be calculated, to provide a more conservative LoD. (Armbruster and Pry, 2008).

2.1.5.1. Limit of Blank (LoB)

Limit of Blank is defined as the highest apparent analyte concentration expected to be found when testing the replicates of a sample which contains no analyte. It is important that although there is no analyte, a blank can produce an analytical signal that might be in accordance with a low concentration of analyte. Detection of LoB is done by measuring replicates of a blank sample and then calculating the mean value and the SD (LoB = mean blank + 1.645(SD_{blank}). Again assuming a Gaussian distribution of the raw analytical signals from blank samples, the LoB represents 95% of the observed values. The other 5% can be a response that could be produced by a sample which contains a very low analyte concentration (Armbruster and Pry, 2008).

2.1.6. Enzyme kinetics

One of the most important approaches in studying the mechanism of enzymatic reactions is to determine the rate of the reaction and how changing experimental parameters influences it. A key factor that affects the rate is the substrate concentration [S], which can be complicated by the fact it changes during *in vitro* reaction because it is converted into product. Usually, kinetic experiments are simplified by measuring initial rate (initial velocity, V_0), when concentration of substrate is much higher than the concentration of an enzyme [E]. If only the beginning of the reaction is monitored, [S] can be regarded as a constant and V_0 can be explored as a function of [S]. In a case when [E] remains constant and [S] is changing, the effect on V_0 is shown in Figure 1. When [S] is low, the slope is almost linear and by increasing [S], the velocity is also increasing proportionally to [S]. Finally, the curve reaches a plateau where velocity is constant. This region is close to maximum velocity, V_{max}. The substrate concentration at ½ V_{max} is the Michaelis constant; K_M (Nelson and Cox, 2012).

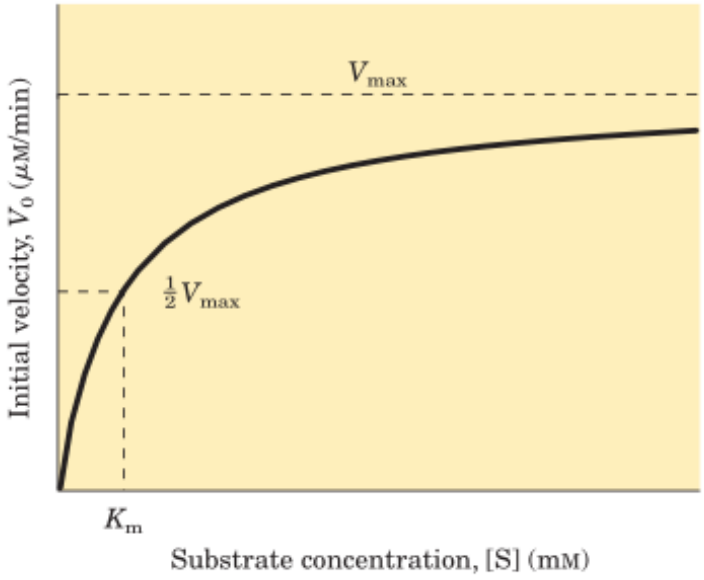

Figure 1. Michaelis-Menten curve of an enzyme reaction showing the relation between substrate concentration [S] and initial velocity (V_0) (Nelson and Cox, 2012).

The curve in Figure 1 has the same general shape as the rectangular hyperbola for most enzymes. It can be expressed algebraically by the Michaelis-Menten equation:

$$V_0 = \frac{V_{max} * [S]}{K_M + [S]} \quad [1]$$

The K_M is often used as an indicator of the affinity of an enzyme for its substrate (Nelson and Cox, 2012).

2.2. LIGNOCELLULOSIC BIOMASS

Lignocellulosic biomass is a renewable resource which can substitute fossil resources for the production of biofuels (Isaksen et al., 2014). There are three different types of lignocellulosic biomass: graminaceous plants (grasses), gymnosperms (softwoods) and angiosperms (hardwoods) (Horn et al., 2012). Nonedible plant material is composed mostly of two polysaccharides: cellulose and hemicellulose. Third major component is lignin, very important phenolic polymer that ensures structural strength to the plant (Sluiter et al., 2010). Apart from latter, there are also minor components such as proteins, soluble sugars, minerals,

lipids and pectin. Three major polymers are interlinked in a hetero-matrix and their abundance varies depending on the type of biomass (Horn et al., 2012).

The percentage of cellulose in natural lignocellulosic biomass is about 25 to 50%, 20 to 40% of hemicellulose and 5 to 35% of lignin. In the plant cell walls, the cellulose fibrils form a skeleton surrounded by hemicellulose and a lignin layer. Because of the plant material and barrier properties of lignin, this biomass cannot be easily degraded (Ioelovich and Morag, 2012). Lignocellulosic biomass structure is visible in Figure 2.

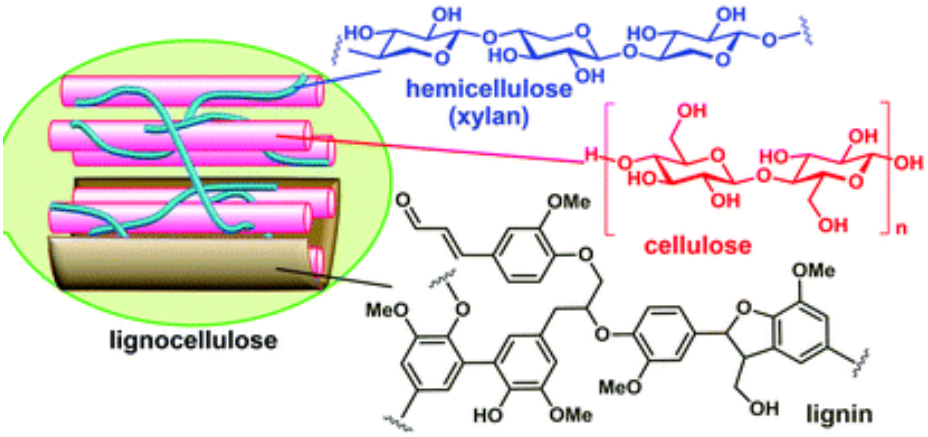

Figure 2. Structure of lignocellulosic biomass (Kobayashi and Fukuoka, 2013).

2.2.1. Cellulose

Cellulose is a linear polysaccharide which consists of hundreds to over ten thousand repeating β-(1,4)-D-glucose units (Figure 3), alternately rotated by 180°, that construct parallel glucans into crystalline microfibrils (Dimarogona et al., 2013). They are connected and stabilized via hydrogen bonds and van der Waals interactions. Microfibrils are non-soluble and therefore hardly accessible for enzymatic saccharification. In spite of that, there is one big advantage of cellulose, its homogeneity, which leads after complete depolymerization to only one product, glucose. (Horn et al., 2012).

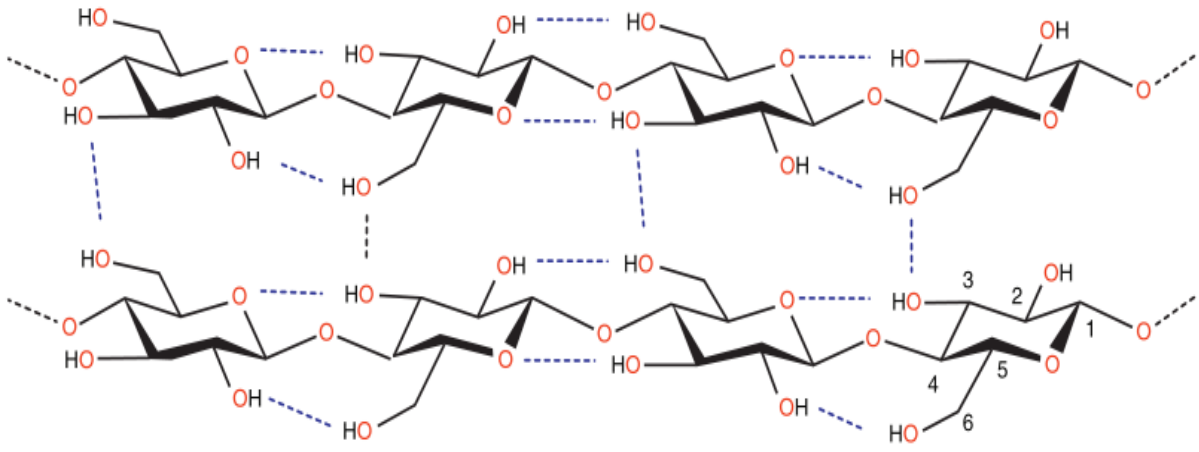

Figure 3. (Partial) structure of cellulose (Hemsworth et al., 2013).

2.2.2. Hemicellulose

Hemicellulose has a large variety, not only between plants, but also even within one plant species and its tissue. It is composed of heterogeneous polysaccharides that contain hexoses (e.g. glucose, mannose), pentoses (e.g. xylose, arabinose) and sugar acids like acetic and galacturonic (Dimarogona et al., 2013). Hemicelluloses degradation is easier for enzymes compared to cellulose, however, some oligomers have complex branching and acetylation patterns which make them recalcitrant. Because of their heterogeneity, depolymerisation of hemicelluloses yields a mixture of different sugars which may contain pentoses that are difficult to ferment. (Horn et al., 2012).

2.2.3. Lignin

Lignin is the name of a group of substances that has large variety depending on different parts and different species of plants and length of growing season. It is a polyphenolic polymer with a three-dimensional network, a complex composed of phenylpropane units linked randomly and nonlinearly. Three main monomers (monolignols) are coniferyl alcohol, sinapyl alcohol and p-coumaryl alcohol. They are incorporated into lignin in the form of guaiacyl (G), syringyl (S) and p-hydroxyphenyl (H), respectively (Figure 4). In lignocellulosic biomass lignin is cross-linked with carbohydrates via e.g. glucuronic acid by ether or ester linkages (Chen, 2014; Horn et al., 2012).

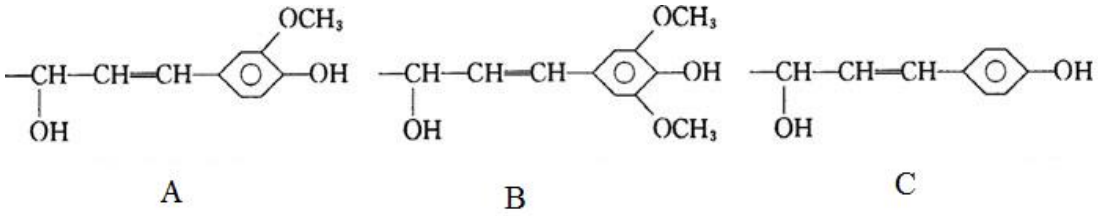

Figure 4. Basic structural units of lignin: A) Coniferyl alcohol, B) Sinapyl alcohol, C) Coumaryl alcohol (Chen, 2014).

2.3. CHITIN

Chitin (Figure 5) is a long chain polymer, crystalline analogue of cellulose, composed of N-acetyl-D-glucosamine (GlcNAc) linearly linked by β-1,4-glycosidic bonds. In its natural form, it is organized in crystalline arrangements that make up robust biological structure like crustacean cuticles. It is also widely distributed in the cell wall of fungi and yeast (Aachman et al., 2012; Dimarogona et al., 2012).

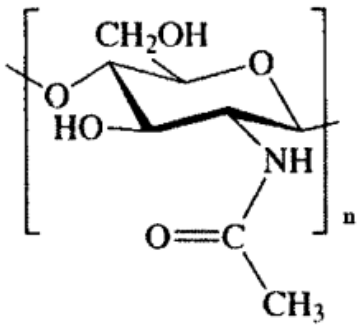

Figure 5. Chemical structure of chitin (Rinaudo, 2006).

2.4. ENZYME CLASSIFICATION

2.4.1. LPMO classification

The CAZy (Carbohydrate Active Enzymes) database (CAZy.org**,** 2017) is a full-scale collection of enzymes acting on carbohydrates together with their carbohydrate-binding modules. They are classified according to their similarities in amino acid sequence (Hemsworth et al., 2015). LPMOs were first classified into carbohydrate-binding module family 33 (CBM33) and glycoside hydrolase family 61 (GH61) (Span and Marletta, 2015). These two families of enzymes are structurally similar and act synergistically with another class of enzymes called cellulases (Forsberg et al., 2011). GH61 largely consisting of fungal enzymes and CBM33 of mainly bacterial proteins (Hemsworth et al., 2015).

After finding that these enzymes catalyze copper-dependent oxidative reactions, the name lytic polysaccharide monooxygenases (LPMOs) was adopted. (Isaaksen et al., 2014). The word "lytic" stands for the ability of these enzymes to break and loosen polysaccharide chains. Because of the importance of this oxidative degradation, CAZy redefined redox carbohydrate active enzymes into a new family with auxiliary activity (AA). GH61 was reassigned as family AA9 and CBM33 as AA10 (Hemsworth et al., 2015).

Based on sequence characteristics, LPMOs are currently categorized as AA9-AA11 and AA13 of the CAZy database. The AA10 family includes mostly bacterial enzymes, but also contains members from eukaryotic organisms and viruses. Several pathogenic bacteria produce AA10 type LPMO domains, which have been identified as virulence factors. Family AA9, AA11 and AA13 almost exclusively contain fungal enzymes (Borisova et al., 2015; Loose et al., 2014). Hemicellulose activity has been described for family AA9, cellulose activity for AA9 and AA10, chitin activity for families AA10 and AA11 and starch activity for family AA13 (Borisova et al., 2015).

Characterization of LPMOs according to their polysaccharide bond preference and amino acid sequence has led to distribution into three types: LPMO-1 (type 1) release reducing end oxidized products (C1 oxidizing enzymes), LPMO-2 (type 2) act on non-reducing end of the glucose moiety (C4 oxidizing enzymes) and LPMO-3 (type 3) releasing both C1 and C4-oxidized cello-oligomers which makes them less specific enzymes (C1 and C4 oxidizing enzymes) (Borisova et al., 2015; Dimarogona et al., 2013).

2.4.2. Cellulases classification

Glycoside hydrolases are a group of enzymes that hydrolyse the glycosidic bond between two or more carbohydrates or between non-carbohydrate and carbohydrate part of the molecule. The nomenclature of enzymes in this group is based on their substrate specificity and molecular mechanism. Cellulases (endo-β-1,4-glucanases) belong to GH Family 5 and GH Family 8. They are responsible for endohydrolisis of β-(1,4)-D-glycosidic bonds in cellulose, lichenin and cereal β-D-glucans (CAZy.org, 2017).

2.5. LPMO STRUCTURES

The first LPMO structures were resolved in 2008 using techniques like X-ray crystallography and NMR. Currently, there are 30 tertiary structures of LPMOs reported in the protein data bank (PDB, 2017); 12 structures are from the fungal AA9 family, 16 structures from the bacterial AA10 family, and 1 structure in each AA11 and AA13 family (CAZy.org, 2017) (Figure 6).

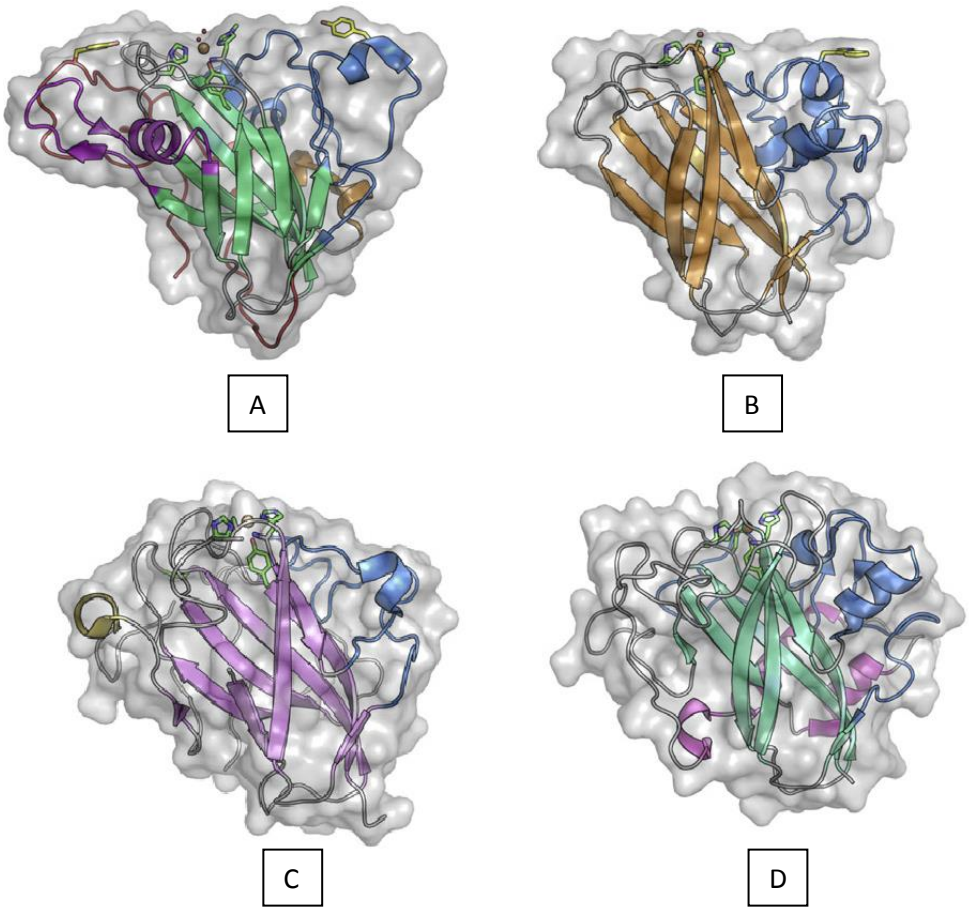

Figure 6. Structural aspects of LPMO: A) AA9, B) AA10, C) AA11, D) AA13 (Hemsworth et al., 2015).

All LPMOs have a similar global structure. The LPMO catalytic domain has a β-sandwich fold that is very similar to the structure of both immunoglobulin (Ig) and fibronectin type III (Fn III) domains (Figure 7). This fold contains disulfide bonds, typically two or three. LPMO domains usually contain 200–250 amino acids, however, the number of residues depends on the cumulative loop length (Span and Marletta, 2015). Structural diversity is generated by the helices and loops that connect the core β-strands, providing variable dimensions and topologies of the substrate-binding surface (Vaaje - Kolstad, 2017).

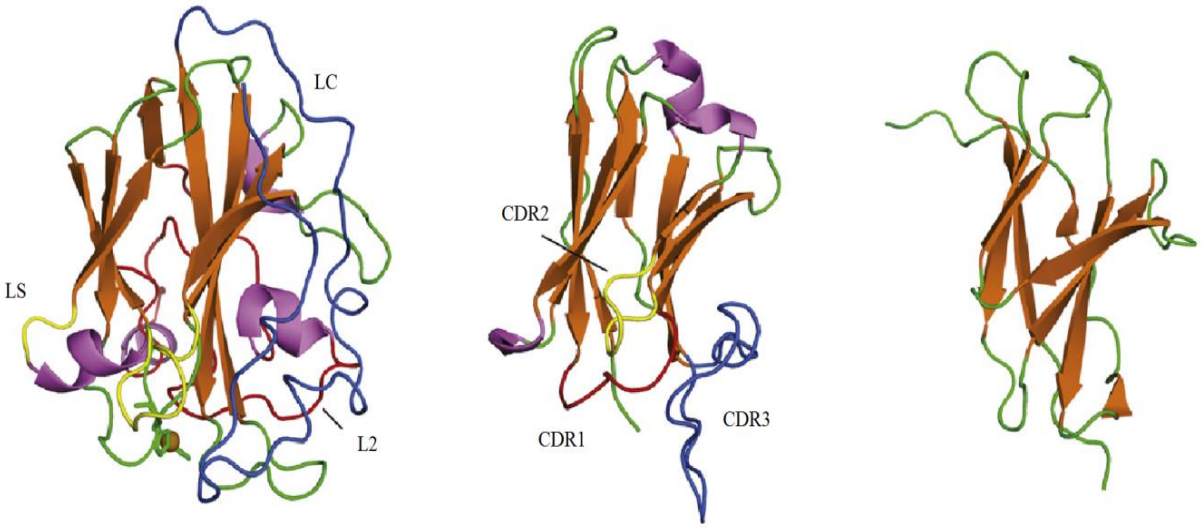

Figure 7. LPMO domain (AA9, *Nc*PMO3) compared to Ig and FnIII domains (Span and Marletta, 2015).

LPMOs active site is positioned at the center of a flat surface, contrary to GH family enzymes, which have substrate-binding grooves or tunnels. Aromatic amino acids which surround the active side are proposed to bind cellulose (Hemsworth et al., 2013). The LPMO active site contains a single copper ion coordinated by the histidine brace which is an unusual arrangement that uses the amino group and sidechain of the N-terminal histidine together with a distal histidine sidechain to coordinate the copper in a T-shaped arrangement of nitrogen ligands. The N-terminal histidine is methylated at Nε residue in fungal LPMOs, while bacterial LPMOs do not have this modification (Span and Marletta, 2015) (Figure 8). Fungal LPMOs expressed in other systems, such as *Pichia pastoris* or *Escherichia coli*, which lack the machinery to make this modification, remain active on polysaccharides notwithstanding the lack of the methylated histidine (Hemsworth et al., 2015.).

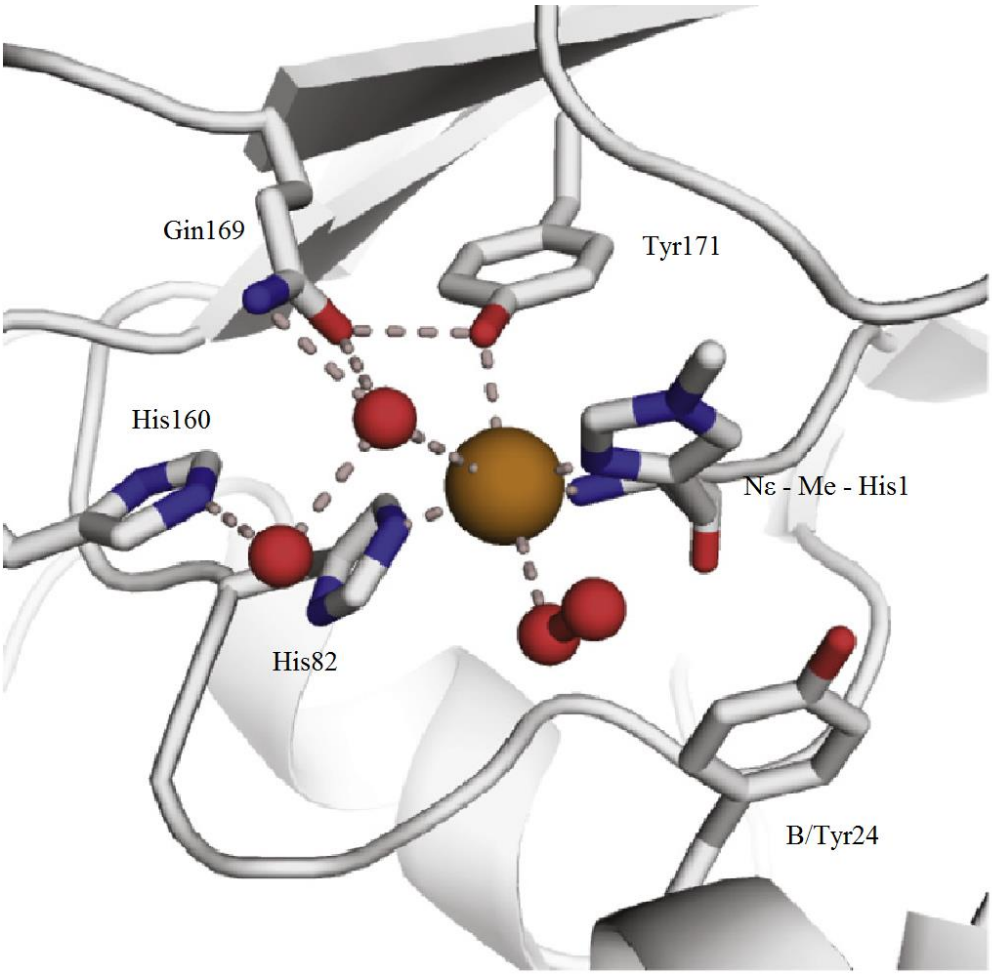

Figure 8. Active site of an AA9 *Nc*PMO3 (Span and Marletta, 2015).

As mentioned above, regioselectivity of enzymes depends on helices and loops that connect the core β-strands, meaning that loop variation is particularly obvious in segments that form the substrate-binding interface. This is thought to be an evolutionary response to selective pressure around substrate availability. In Figure 7 three different loops are visible: L2 loop/motif 1 (red), LC loop (blue) and LS loop (yellow) (Span and Marletta, 2015).

There are differences in structures of oxidized and reduced active site of LPMOs. In oxidized LPMOs, Cu(II) is coordinated by additional ligands in a distorted trigonal and octahedral bipyramidal geometry. Up to three additional ligands are oxygen atoms either from water, molecular oxygen or the axial tyrosine. In reduced LPMOs, coordination numbers are decreased consistent with Cu(I) coordination preferences. All LPMO families studied for now have conserved active-site hydrogen-bonding residues that interact with active-site water molecules and the active-site tyrosine ligand, if it is present (Span and Marletta, 2015). Bacterial LPMOs have different structure than fungal and their apical sites are not occupied by an oxygen atom from a water molecule or tyrosine as in fungal, but by alanine and

phenylalanine which are limiting the copper ion coordination to equatorial sites only (Dimarogona et al., 2013). Few functions are suggested for these residues such as hydrogen-bonding to a substrate bound in the available equatorial position, modification of the electronic environment of the copper center and stabilization of the second histidine ligand (Span and Marletta, 2015).

2.6. LPMO ACTIVITY

All LPMOs that were characterized showed activity either on cellulose or on chitin, indicating that these enzymes act on highly crystalline structure. Because of the fact that LPMOs are co-secreted by microorganisms that are included in biomass degradation and because of a wide variety of the sequences among LPMOs, it is hard to believe that these two are the only substrates for LPMOs (Agger et al., 2014). In further investigations it was shown that LPMOs are active not only on cellulose or chitin, but also on xylan, xyloglucan, glucomannan, lichenan, β-glucan, and starch (Span and Marletta, 2015).

For catalyses, these enzymes required molecular oxygen as well as reducing agents. Electron donors can be small molecule reductants such as ascorbic or gallic acid, or enzymes such as cellobiose dehydrogenase (CDH), which are very often co-expressed with LPMOs (Isaksen et al, 2014). It is believed that oxidation leads to polysaccharide chain cleavage introducing new chain-ends. First, the copper atom is reduced and molecular oxygen is activated by LPMOs. Afterwards the copper-oxygen complex is able to attack the hydrogen either of the C1 or C4 of the glycosidic bond resulting in abstraction of the hydrogen and afterwards hydroxylating the carbon by the -OH group. The strength of the C-H bond is estimated to be at least 95 $kcalmol^{-1}$. After hydroxylation at that position, an elimination reaction occurs which lead to destabilization and bond breakage of the glycosidic bond. This is an irreversible reaction because the carbon on the reducing or non-reducing ends had been oxidized (Beeson et al., 2011; Frandsen et al., 2016). Products of the reaction are oxidized oligosaccharides and native oligosaccharides that contain reducing ends originally present in the polymeric substrate. Products oxidized at C1 are initially in lactone form, which is then hydrolyzed spontaneously or enzymatically into aldonic acid. It can be phosphorylated into gluconic acid which can be metabolized by pentose phosphate biochemical pathway. If substrates are oxidized at C4, 4-ketoaldose is generated if the same general mechanism as for the C1 oxidation is proposed, but oxidation at the non-reducing end is more difficult to

analyse (Beeson et al., 2011) (Figure 9). Mass spectrometry was done, and both oxidation at C4 and C6 has been suggested. *Nc*LPMO9D was used generating products for which it has been shown that oxidation at C4 is happening rather than at C6. That was demonstrated by Isaksen et al., 2014. It can be concluded that cellulose cleavage at position 1 or 4 is energetically favored since it occurs through a simple elimination reaction, while oxygen insertion at other sites would require the cooperation of additional amino acids for glycosidic bond cleavage (Dimarogona et al., 2012).

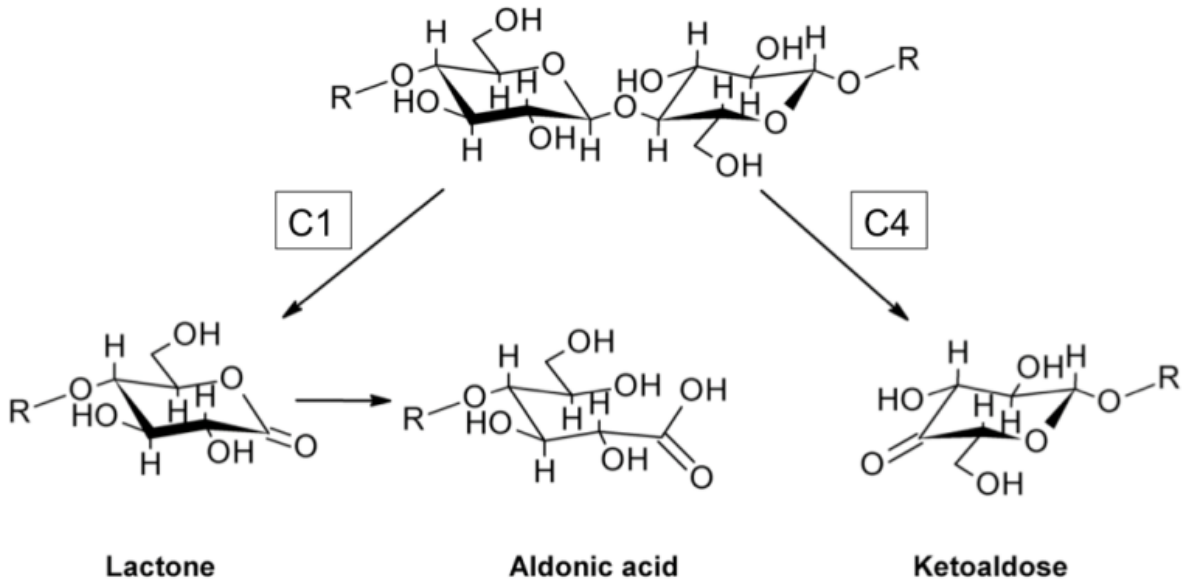

Figure 9. Oxidized reaction products generated from AA9 applied on cellulosic substrates (Hemsworth et al., 2012).

Today, it is widely accepted that a microbial oxidoreductive cellulose degrading system exists in parallel with the long-known hydrolytic cellulase system (Dimarogona et al., 2012). It was shown that LPMOs cleave glycosidic bonds, contain a copper in the active site and need reducing agent for initiation of their activity. LPMOs accept electrons from many different sources such as X-ray beam used for crystallography and light-excited pigments. Reducing agents can also be naturally occurring in the substrate (gallic acid, lignin), added externally (ascorbic acid, glutathione), in the form of phenolic compounds, but can also be an

enzyme, such as cellobiose dehydrogenase (CDH). CDHs are often encoded by wood degrading fungi and act as an electron donor to AA9. It is even discovered that CDH is also able to activate *Neurospora crassa* AA13 to attack starch (Hemsworth et al., 2015). It consists of two domains (N-terminal heme domain which carries a cytochrome *b* type heme and C-terminal flavin domain which contains FAD, connected via flexible linker) and catalyzes the two-electron oxidation of cellobiose (the product of cellobiohydrolases) to cellobionolactone, while also generating hydrogen peroxide. Oxidation of cellobiose occurs in the flavin domain with subsequent electron transfer to the heme domain (Johansen et al., 2016; Philips et al., 2011). The CDH/LPMO system was shown to improve the degradation of cellulose in combination with cellulases (Kittl et al., 2012). During CDH reaction, the Cu(II) center must be reduced into Cu(I) before activating O_2. It is suggested that $FADH_2$ is re-oxidised to FAD, electrons are shuttled from CDH via its cytochrome domain to AA9, presumably reducing Cu(II) to Cu(I), that makes LPMO active. In the proposed mechanism, CDH is interacting with a patch on the side of AA9 and electrons are passed via its cytochrome domain along wires of hydrophilic side chain within the core of the LPMO leading to the copper active side (Hemsworth et al., 2015). After that, oxygen activation, hydrogen-atom abstraction (HAA) and oxygen insertion, on the substrate carbon occurs. There are two possible scenarios, in one HAA and oxygen insertion are happening before the second reduction and in this case direct ET (electron transfer) requires binding of LPMO and substrate and dissociation in between the two reductions. Second scenario is that second reduction happens before HAA, however, in this case direct ET would still require the LPMO traveling back and forth between substrate and redox partner CDH. For bacterial LPMOs ET pathways have not been clear yet because bacteria do not contain CDH and therefore completely depend on other electron donors, like reductants. All in all, the LPMO domain looks perfect for LPMO catalysis; it contains the core with conserved ET-competent residues, the loops for substrate binding. It is presumed that components closer to the active site help in binding oxygen and directing electrons and protons to the reactive intermediate (Span and Marletta, 2015). The concerted activity of LPMOs and CDHs in oxidative cleavage of cellulose should not be overestimated, because not all organisms have genes encoding for both enzymes in their genomes. (Dimarogona et al., 2012). In addition to CDH, single-domain flavoenzymes such as glucose dehydrogenase and aryl-alcohol quinone oxidoreductases can also play an important role of electron donors for LPMOs (Johansen, 2016).

2.6.1. H_2O_2 as a co-substrate

H_2O_2 represents a potentially efficient way to supply the protons, electrons and oxygen that are needed for the 'monooxygenase' reaction and is naturally present in ecological niches where plant biomass decomposition occurs and LPMOs are present (Bissaro et al., 2017). By using enzyme assays, mass spectrometry and experiments with labeled oxygen atoms, it is shown that H_2O_2, and not O_2 as previously thought, is the co-substrate of LPMOs. A catalytic mechanism in which an H_2O_2-derived oxygen atom, rather than one derived from O_2, would be introduced into the polysaccharide chain is suggested. In that mechanism, first occurs priming reduction of the Cu(II) to Cu(I) in the catalytic center of the enzyme. H_2O_2 is then binding to the Cu(I) and homolytic bond cleavage would produce a hydroxyl radical. It is thought that this leads to Cu(II)-hydroxide intermediate formation and a substrate radical. Eventually, the reaction between copper-hydroxyl intermediate and the substrate radical leads to substrate hydroxylation and regeneration of the Cu(I) center which is then able to perform a new catalytic cycle (Bissaro et al., 2016). Addition of exogenous H_2O_2 alone did not lead to cellulose oxidation, however, had a positive effect on LPMO activity when a reductant was also added. Furthermore, high concentrations of H_2O_2 inactivate the enzyme. If H_2O_2 is added responsibly, an initial increase in LPMO activity is revealed at lower H_2O_2 concentrations and progressively rapid enzyme inactivation with increasing H_2O_2 concentration. It is also proven that oxidases can induce LPMO activity if a reductant is available. In this matter, abundant phenols derived from plants and fungi have recently been implicated in the reductive activation of LPMOs (Bissaro et al., 2017).

2.6.2. 2,6-dimethoxyphenol (DMP)

Polyphenols are largely present in plant in the form of monomers or polymers structures. They are limited for use because of their lower solubility and stability. 2,6-dimethoxyphenol is a monophenolic compound that is used for the measurement of laccase (EC 1.10.3.2) and peroxidase (EC 1.11.1.7) activity. Laccases are multi-copper-containing enzymes, which reduce molecular oxygen to water and simultaneously perform one-electron oxidation of various substrates such as diphenols, methoxy-substituted monophenols, etc. (Adelakun et al., 2012). Peroxidases are heme proteins with histidine as ligand. The iron in the resting enzyme is Fe(III). They use two phenolic electron donors to reduce H_2O_2 into two

water molecules (CAZy.org, 2017). The mechanism for the oxidation of DMP catalyzed by laccases and peroxidases was suggested and it is shown in Figure 10. Two DMP molecules are oxidized at the hydroxyl group, two electrons are transferred to the electron acceptor (manganese, iron, copper) and further reduction of hydrogen peroxide to two water molecules occurs. The two DMP phenoxy radicals spontaneously dimerise to hydrocoerulignone, which is again an electron donor. One hydrocoerulignone is oxidized to one coerulignone under reducing hydrogen peroxide to water. Coerulignone (oxidized DMP quinone dimer) shows a strong absorptivity at 469 nm. In the reaction two DMP molecules are oxidized under reduction of two H_2O_2 molecules with a stoichiometry of 2:1 for DMP:H_2O_2. (Wariishi et al., 1992).

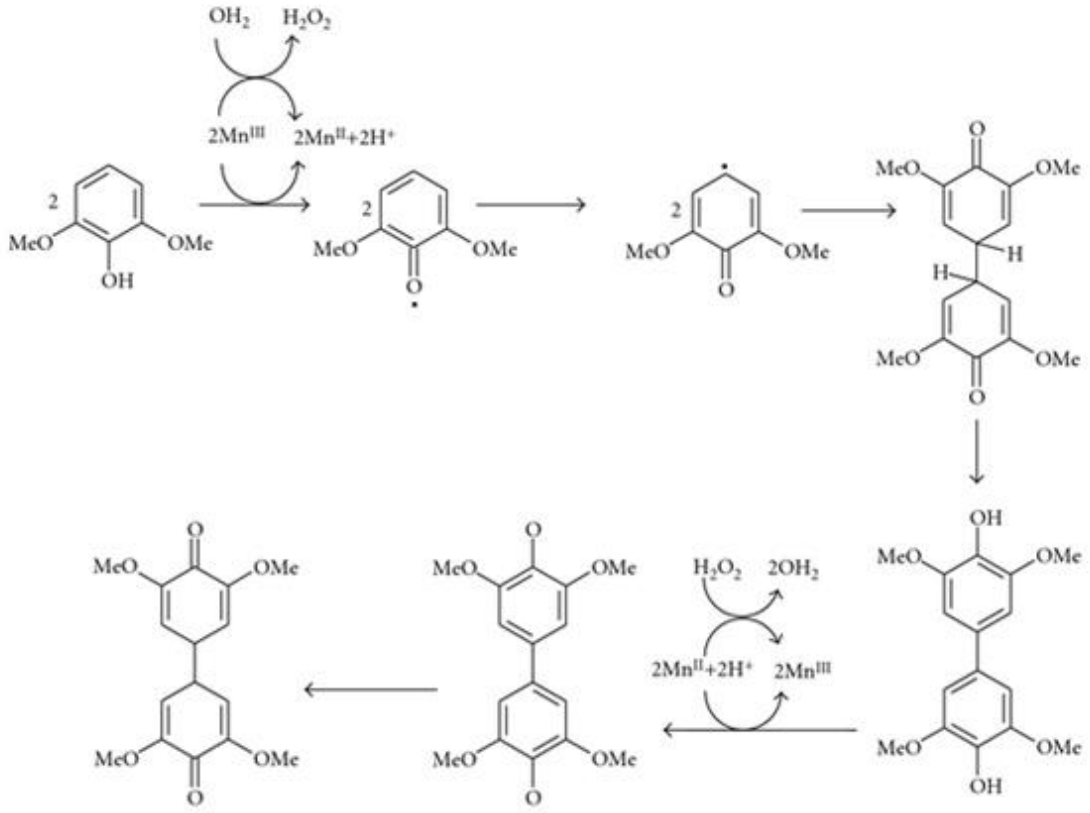

Figure 10. Proposed mechanism for oxidation of 2,6-dimethoxyphenol catalyzed by manganese peroxidase (Wariishi et al., 1992).

Since we know that H_2O_2 is a co-substrate for LPMO, all phenolic compounds reacting less with LPMO and not showing activity in a spectrophotometric assay, should be re-tested if the reactivity in the presence of H_2O_2 instead of only O_2 is increased. The advantage of chromogenic compounds like DMP, which is already well studied, to measure the activity of LPMO in such a spectrophotometric assay is big.

In this graduate thesis we show that DMP reacts with LPMO and H_2O_2 as a co-substrate and that it is suitable to develop a fast and sensitive spectrophotometric assay to easily detect activity for characterization of LPMOs.

3. MATERIALS & METHODS

3.1. ENZYME

The enzyme that was used in the experiments is lytic polyssacharide monooxygenase (LPMO - 02916) isolated from fungi *Neurospora crassa*.

3.2. CHEMICALS

Chemicals that were used for all assays are listed in the Table below. All chemicals used were of analytical grade or highest purity available.

Table 1. Chemicals used in assays and their sources.

Assay	Chemical	Source
Substrate screening	Sinapic acid Pyrochatechol Gallic acid 2,6-dimethoxyphenol	Sigma Aldrich (St. Louis, USA)
Basic assays	EDTA Copper(II) sulfate Copper(II) chloride	Sigma Aldrich (St. Louis, USA)
pH profile	**1. Anionic buffers:** Acetic acid Malic acid Phosphoric acid Dimethylarsinic acid Succinic acid Citric acid	 Fluka (St. Gallen, CH) Roth (Karlsruhe, Germany) Sigma Aldrich (St. Louis, USA)
	2. Kationic buffers: Pyridine Imidazol 2,4-dimethylimidazol Histidine	 Sigma Aldrich (St. Louis, USA)

In all experiments two substrates were used: 2,6-dimethoxyphenol (DMP) as a chromogenic substrate and hydrogen peroxide (H_2O_2) as co-substrate, both from Sigma Aldrich (St. Louis, USA).

All aqueous solutions were prepared using reverse osmotic water (RO-H_2O) or water purified and deionized (di-H_2O, 17 MΩ cm) with a HQ water system (Ultra Clear basic UV, SG, Siemens, Berlin/Munich, Germany).

3.3. SUBSTRATE SCREENING

In order to determine the most suitable chromogenic substrate for all characterization assays, the substrates sinapic acid, pyrochatechol, gallic acid and DMP were screened.

The screening was done at room temperature (~23°C). UV/Vis spectra were recorded with an Agilent 8453 UV–visible spectrophotometer equipped with a photodiode array detector (Figure 11). Concentrations of LPMO, hydrogen peroxide and substrates were 2 μM, 100 μM and 0.2 mM, respectively. A 100 mM pH 6.0 buffer combining succinic acid and phosphoric acid to cover a broader stable pH range (pH 4.5–pH 8.0) was used. As a control experiment all assays were performed without adding H_2O_2 (water was added to reach the same volume).

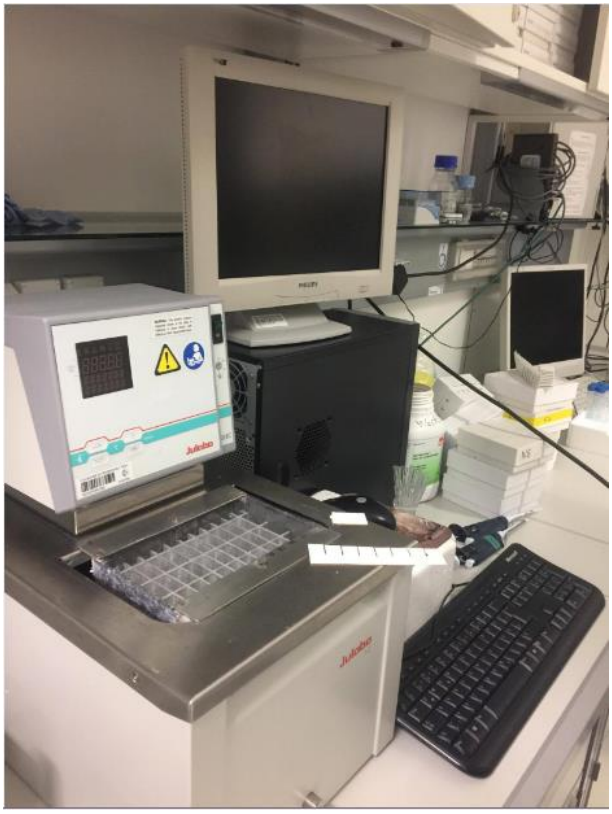

Figure 11. Agilent 8453 UV–visible spectrophotometer.

3.4. CHARACTERIZATION - VOLUMETRIC AND SPECIFIC ACTIVITY

LPMO activity was measured at 30°C by monitoring the oxidation of 1 mM 2,6-dimethoxyphenol (DMP) in 100 mM succinic-phosphoric buffer at pH 7.5. The absorption maximum of oxidised DMP which forms coerulignone (the chromogenic endproduct) is at 469 nm and the corresponding extinction coefficient is ε_{469} = 49.6 $mM^{-1}cm^{-1}$ (Wariishi et al., 1992). Cuvettes with a volume of 1 mL and 1 cm path length (d) were used to measure the kinetic slope over time, to further calculate the volumetric activity in units per milliliter. The enzyme activity is usually defined as amount of substrate converted to product per time unit. According to the SI system, concentration of product must be in mol and time in seconds. The enzyme unit 1 katal is defined as the amount of enzyme converting 1 mol substrate forming 1 mol product in one second. However, besides katal, international unit is more often used (Bisswanger, 2014). One unit of enzymatic activity is defined as the amount of enzyme to produce one micromole chromogenic product per minute (1U = 1 $\mu molmin^{-1}$). The enzyme factor was calculated by dividing the extincion coefficient with a factor of 2 (ε_{469} = 24.8 mM^{-1} cm^{-1}), considering coerulignone is a dimer. The calculation was done by multiplying the kinetic slope with the enzyme factor and the dilution of enzyme.

Enzyme factor was calculated with following formula:

$$EF\ [s^{-1}] = \frac{total\ volume\ [mL]\ *60}{enzyme\ volume\ [mL] * d\ [cm] * \varepsilon\ [mM^{-1}cm^{-1}]} = 60.5\ s^{-1}\ for\ DMP \qquad [2]$$

After the volumetric activity, specific activity was also calculated by dividing volumetric activity with concentration of the *Nc*LPMO_02916 which is 51.75 $mgmL^{-1}$.

3.4.1. Standard LPMO activity assay

860 µL succinic-phosphoric buffer, pH 7.5, concentration 116 mM, 20 µL LPMO, concentration 25 µM, 20 µL H_2O_2, concentration 5 mM and 100 µL DMP, concentration 10 mM were added in cuvette to get the final concentrations of buffer 100 mM, LPMO 0.5 µM, H_2O_2 100µM and DMP 1mM. Everything was mixed and measurement lasted for 300 s.

3.4.2. Control experiments

Different assays were performed in the same way as in the standard assay, apart from adding 100 µL of water instead of the DMP (effect of no substrate), 20 µL of water instead of H_2O_2 (effect of no co-substrate) and 20 µL of buffer for enzyme dilution (10 mM succinic-phosphoric buffer) instead of LPMO (effect of no enzyme).

3.4.3. $CuSO_4$ and $CuCl_2$ instead of LPMO

Different standard assays were performed by exchanging the enzyme (LPMO) either with copper(II)sulfate ($CuSO_4$) or copper(II)chloride ($CuCl_2$) with tree different concentrations of copper (0.5 µM, 5µM and 50 µM). To see the effect of the co-substrate, the standard assay with $CuSO_4$ instead of LPMO was also performed without H_2O_2.

860 µL succinic-phosphoric buffer, pH 7.5, concentration 116 mM and 100 µL DMP, concentration 10 mM were added in every assay. Final concentrations in cuvettes were: buffer 100 mM and DMP 1mM. Everything was mixed and measurement lasted for 300 s.

3.4.4. Stability assays

In order to define stability of the LPMO, assays with ethylenediaminetetraacetic acid (EDTA) and heat inactivated LPMO were done. The absorbance was measured for 300 s at the Diode array.

For the heat test four solutions were made in eppendorf tubes by adding 1075 µL of succinic-phosphoric buffer, pH 7.5, concentration 100 mM and 25 µL LPMO, concentration 0.5 µM. Eppendorf tubes were vortexed and then transferred into a heating block at 100°C for 30 minutes, 60 minutes, 2 hours and 4 hours. After the incubation, eppendorf tubes were put on ice and 880 µL of each enzyme solution were transferred into a cuvette. Reaction was started by adding 20 µL of H_2O_2, concentration 50µM and 100 µL of DMP, concentration 1 mM.

There were two different concentrations of EDTA included in the stability test: 1 mM and 2 mM. EDTA solution was prepared with original stock of EDTA disolved in 10 mM succinic-phosphoric buffer at pH 6.0. LPMO (final concentration 0.5 µM) was added and incubated for 30 minutes. 860 µL of succinic-phosphoric buffer at pH 7.5, concentration 116

mM (final concentration 100 mM); 20 µL 5 mM H_2O_2 (final concentration 100µM) and 100 µL 10 mM DMP (final concentration 1 mM) were added in the cuvette which was completed by adding 20 µL of EDTA and LPMO solution.

3.4.5. pH profile

Two types of pH-profiles were done, with anionic and kationic buffer species. Anionic buffers were prepared from acetic acid, succinic acid, malic acid, citric acid, dimethylarsinic acid and phosphoric acid and assays were done in a pH range from 3.5 to 8.5. Kationic buffers were prepared from pyridine, imidazol, 2,4-dimethylimidazol and histidine in a pH range from 4.0 to 9.5. All buffers were prepared by diluting mentioned compounds in highly pure water.

The relationship between pH and the buffer components is described by Henderson-Hasselbach equation:

$$pH = pK_a - log \frac{[HAc]}{[Ac^-]} \quad [3]$$

pH = - log $[H^+]$; negative logarithm of the proton concentration
pK_a = - log K_a; negative logarithm of K_a, the dissociation constant of buffer components
HAc = acid in the non-dissociated form
Ac^-= acid in the dissociated form

The pK_a value is very important since that value indicates pH at which buffer is half dissociated and shows the highest buffer capacity. The capacity range of buffer is narrow and includes two pH units at best (Bisswanger, 2014). For that reason, before deciding which buffer species should be used, pK_a values of kationic and anionic buffer compounds have to be checked in order to decide which pH range can be covered. When analyzing the pH dependence of an enzyme, a broader pH range is required, so several buffer systems may be combined (Bisswanger, 2014). This is the reason of using numerous buffers in the pH profile assays.

In measuring cuvettes 100 mM buffer, 25 mM DMP and 100 µM H_2O_2 were mixed to a total volume of 980 µL. 20 µL LPMO was added in the end to start the reaction. For all buffers different concentrations of the enzyme were used to reach a reliable activity. The change in absorbance over time was recorded with a UV/Vis photometer (Lambda 35, Perkin

Elmer, USA) (Figure 12) and measurement lasted for up to 30 seconds. Measurements were done in single cuvettes to use initial rates (2-5 sec) for slope calculation.

Figure 12. Spectrophotometer Lambda 35 with water bath.

After measuring kationic and anionic buffers, we chose the most suitable combined buffer system in a broad pH range. The anionic buffer system was succinic acid-phosphoric acid buffer. Two solutions were prepared, succinic acid and sodium hydrogen phosphate (NaH_2PO_4) were separately dissolved in highly pure water, each of them 50 mM to reach an 100 mM end concentration of buffering species. Same procedure was done in order to prepare pyridine-imidazol buffer for the kationic buffer system. In these two measurements the pH range was 4.5 to 8.0. Concentration and volume of the buffers and H_2O_2 in the cuvettes were the same as in the assays mentioned above.

3.4.6. Temperature effect

The change in absorbance during time was measured with Agilent 8453 UV–visible spectrophotometer equipped with a photodiode array detector. Using the standard assay the effect/influence of temperature regarding assay stability/enzymatic activity was tested by incubating the assay solutions (without enzyme) at different temperatures in a water bath for 30 minutes. Nine different incubation temperatures were tested and controlled with a

thermometer in the cuvettes: room temperature, 25°C, 30°C, 35°C, 40°C, 45°C, 50°C, 55°C and 60°C. After incubation, reaction was started by adding 0.5 μM LPMO.

Apart from calculating volumetric and specific activity, Arrhenius equation to calculate the activation energy of the reaction was used:

$$ln\, k = ln\, A - \frac{E_a}{R} * \frac{1}{T} \quad [4]$$

k = rate constant [Ug^{-1}]
A = pre-exponential factor, a constant for each chemical reaction
E_a = activation energy for the reaction [$kJmol^{-1}$]
R = universal gas constant; 8.314 [$Jmol^{-1}K^{-1}$]
T = absolute temperature [K]

The natural logarithm (ln) of the specific activity [Ug^{-1}] was plotted versus the inverse temperature (1/T). The slope in the linear range multiplied by the gas constant is equal to the activation energy.

3.4.7. Kinetic constants - K_M and V_{max} values

K_M and V_{max} values for both DMP and H_2O_2 were measured with UV/Vis photometer (Lambda 35, Perkin Elmer, USA). Assays for each substrate were made in 100 mM succinic-phosphoric buffer both at pH 6.0 and pH 7.0.

In order to determine K_M and V_{max} values for DMP and H_2O_2, eight concentrations of DMP (0.5 mM, 1 mM, 2 mM, 10 mM, 25 mM, 50 mM, 85 mM and 115 mM) and six concentrations of H_2O_2 (2 μM, 5 μM, 25 μM, 100 μM, 300 μM and 1000 μM) were used.

LPMO concentration at pH 6 was 1.5 μM, and in the case of pH 7 it was 0.10 μM.

In addition, kinetic constans for H_2O_2 were also measured at pH 7.5. In this case eight different concentrations of H_2O_2 could be used: 2 μM, 5 μM, 10 μM, 25 μM, 50 μM, 75 μM, 100 μM, 500 μM with only two concentrations of DMP: 0.5 mM and 1 mM. In this assay LPMO concentration was 0.01 μM.

3.4.8. Limit of Detection

Before carrying out this test, the lowest LPMO concentration which gives a three times higher linear slope compared to the noise had to be determined. In order to do this, a few different LPMO concentrations were measured using the standard assay.

After finding out the approximately lowest activity range of the reaction, it was decided that the highest concentration is D0 (dilution zero, original stock for the assay) and the lowest one is D800 (dilution 1:800). Twelve different concentrations of LPMO were made in between to cover the whole range (for example, D80 means 1:80 dilution, D200 1:200 dilution, etc.). LPMO concentrations are listed in the table below (Table 2).

Table 2. Symbols for the dilutions and their LPMO concentrations.

DO	10 μM
D2	5 μM
D4	2.5 μM
D8	1.25 μM
D10	1 μM
D20	0.5 μM
D40	0.25 μM
D80	0.125 μM
D100	0.1 μM
D200	0.05 μM
D400	0.025 μM
D800	0.0125 μM

For this assay, two dilution series were carried out containing twelve dilutions. D10 and D100 were made directly from D0 using at least 10 μL of it. D2, D4 and D8 were made from D0; D20, D40 and D80 were made from D10 and D200, D400 and D800 were made from D100 in order to avoid as much mistakes as possible. The dilutions of LPMO were made in 10 mM succinic-phosphoric buffer at pH 6.0. Everything was vortexed before the assay was started. A randomized measuring scheme for all dilutions was made in an excel file (Table 3). The numbers from 1 to 6 are showing which 8 dilutions are used in which measurement because 8 cuvettes were measured at once.

Table 3. Measuring scheme for determination of LoD.

Dilution 1		Dilution 2		
D800	D20	D100	D8	1
D200	D200	D200	D2	
D2	D800	D80	D200	2
D8	D10	D20	D0	
D100	D0	D800	D100	3
D0	D100	D10	D800	
D400	D40	D8	D40	4
D10	D400	D400	D20	
D40	D8	D2	D400	5
D20	D2	D4	D4	
D80	D80	D40	D80	6
D4	D4	D0	D10	

All 48 cuvettes were incubated at 30°C for 10 minutes. For every measurement 8 cuvettes were used and LPMO dilutions were added according to the scheme in Table 3.

4. RESULTS & DISCUSSION

4.1. SUBSTRATE SCREENING

Results of substrate screening are shown below from Figure 13-16. All experiments were done spectrophotometricaly and with and without hydrogen peroxide.

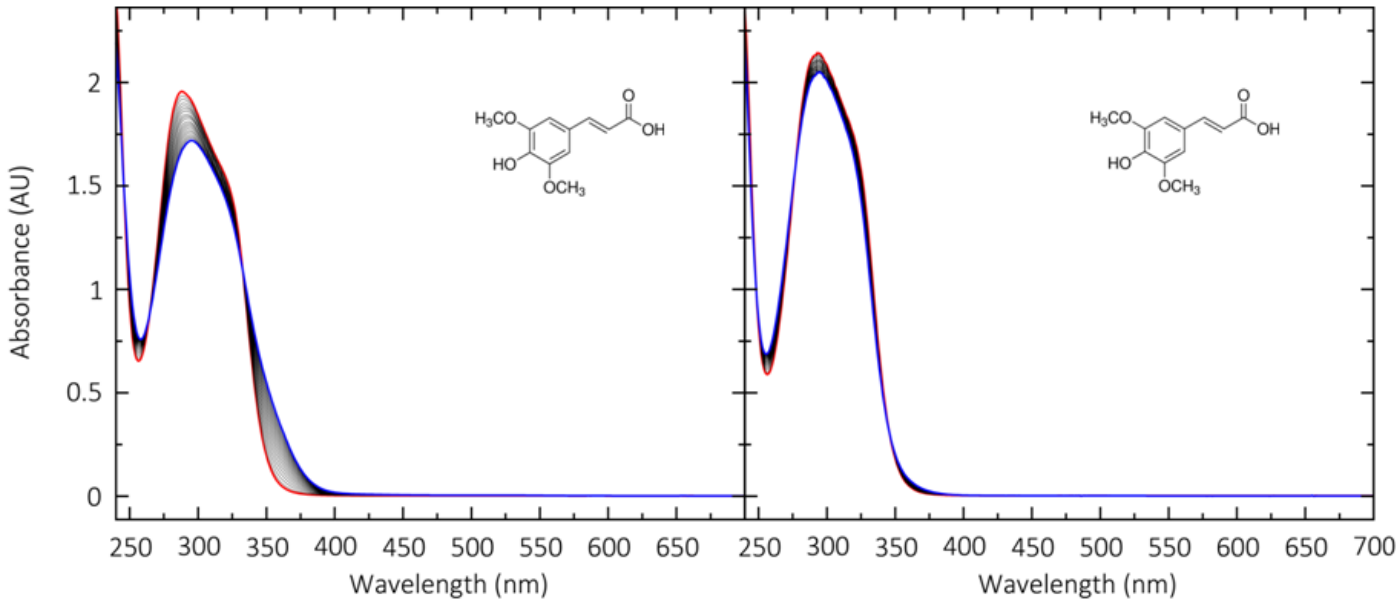

A B

Figure 13. Spectra of sinapic acid together with its chemical structure over time; red line shows initial spectra and blue line shows spectra after 5000 s. A) Assay done with buffer, sinapic acid, LPMO and H_2O_2, B) Assay done with buffer, sinapic acid, LPMO and <u>without</u> H_2O_2.

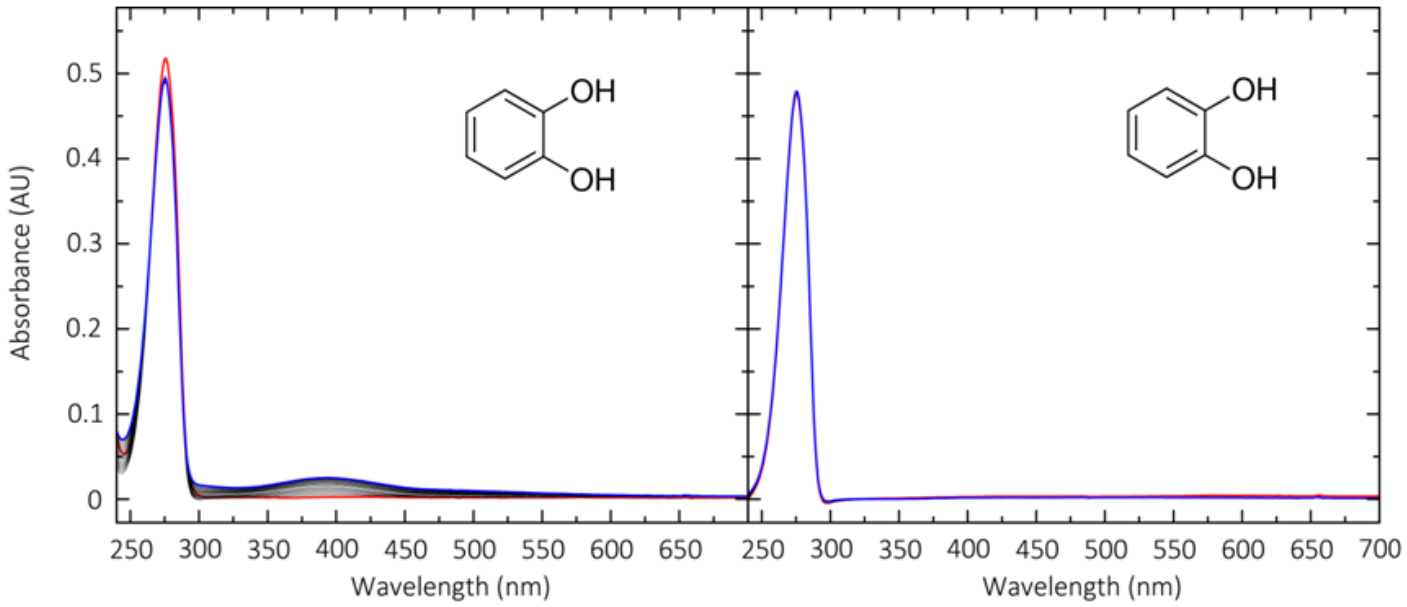

Figure 14. Spectra of pyrocatechol together with its chemical structure over time; red line shows initial spectra and blue line shows spectra after 2500 s. A) Assay done with buffer, pyrocatechol, LPMO and H_2O_2, B) Assay done with buffer, pyrocatechol, LPMO and without H_2O_2.

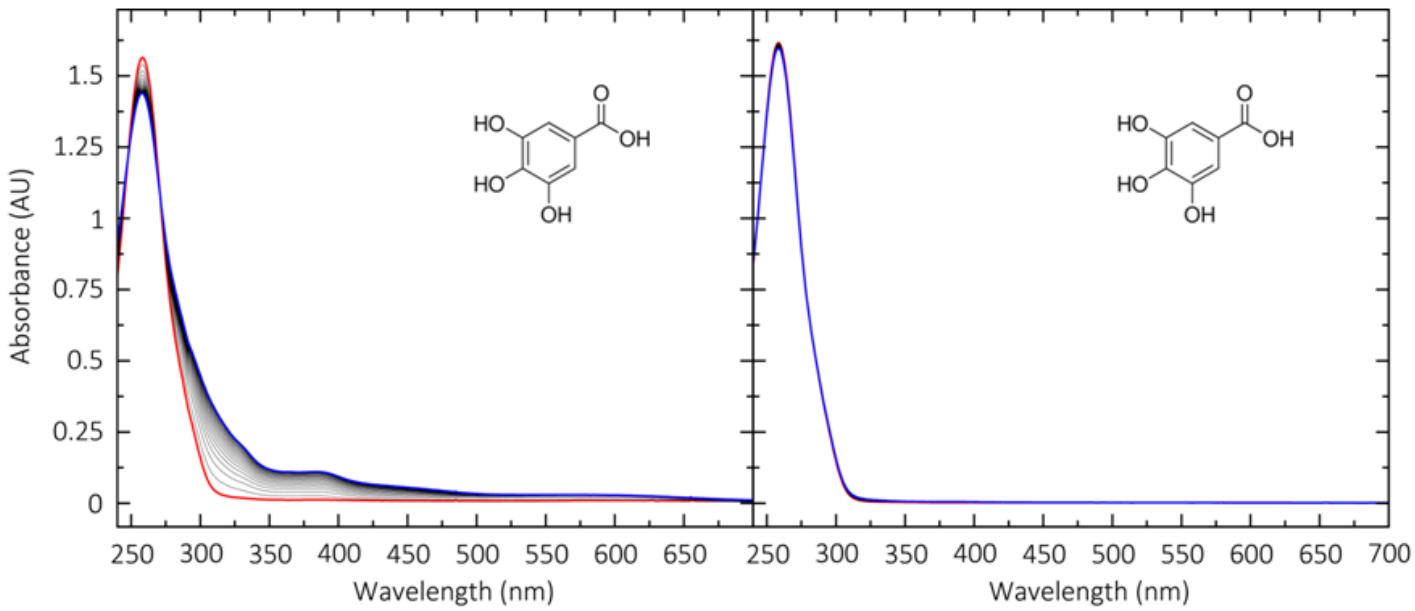

Figure 15. Spectra of gallic acid together with its chemical structure over time; red line shows initial spectra and blue line shows spectra after 2500 s. A) Assay done with buffer, gallic acid, LPMO and H_2O_2, B) Assay done with buffer, gallic acid, LPMO and without H_2O_2.

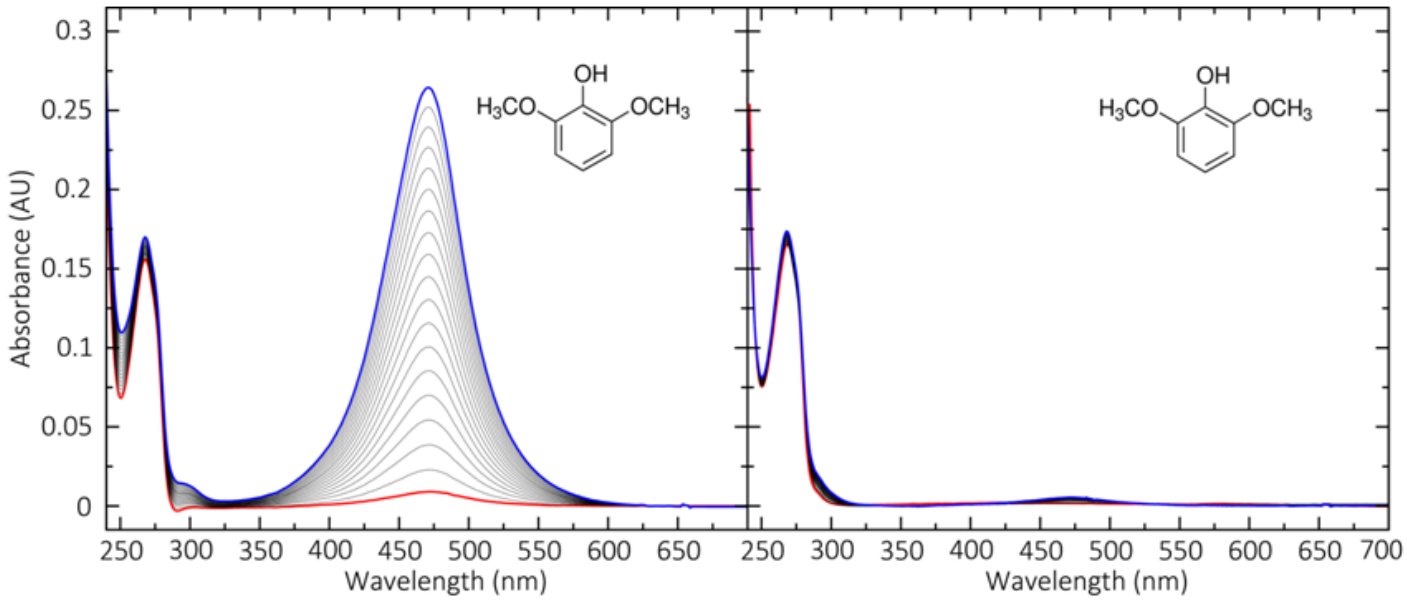

Figure 16. Spectra of DMP together with its chemical structure over time; red line shows initial spectra and blue line shows spectra after 5000 s. A) Assay done with buffer, DMP, LPMO and H_2O_2, B) Assay done with buffer, DMP, LPMO and <u>without</u> H_2O_2.

Two things are similar for all tested substrates. First, we see a peak in the ultraviolet range, which results from the double bonds in the aromatic ring and is typical for phenolic compounds. In the measurements with H_2O_2, during reaction (oxidation) an increase and decrease in absorbance can be observed. The decreasing absorbance at the initial peak maxima and the occurring peak or peak shift shows the oxidation of substrate and the accumulation of the oxidation product. This could be either a stable phenoxy radical, a dimerized or polymerized product.

Sinapic acid shows a shift in absorption around 360 nm, pyrocatechol 390 nm, gallic acid around 325 nm and a peak at 370 nm, pyrocatechol shows a peak at 390 nm and DMP at 469 nm. It is also visible that DMP is showing the highest peak.

Secondly, without using H_2O_2 in the reaction, we do not see any change in the spectra's after the same time. This is an indication that H_2O_2 plays an important role for LPMO activity and might be its co-substrate rather than O_2. It is obvious that the reaction with DMP and H_2O_2 is showing the highest change in absorbance compared to the reaction without H_2O_2. The calculated rate (absorbance increase over time) is 63 times higher in the case of using H_2O_2. Furthermore, the DMP peak occurs in the visible range, which makes it very

useful as a substrate for enzymatic activity assays. Due to these facts we decided to use DMP as chromogenic substrate to develop an activity assay for LPMOs.

4.2. BASIC LPMO ASSAYS

4.2.1. Negative assays for LPMO

It should be proven that DMP and H_2O_2 are both important for LPMO activity and that, on the other hand, nothing will happen if these two compounds are added into the cuvette without LPMO. Results are shown in Figure 17.

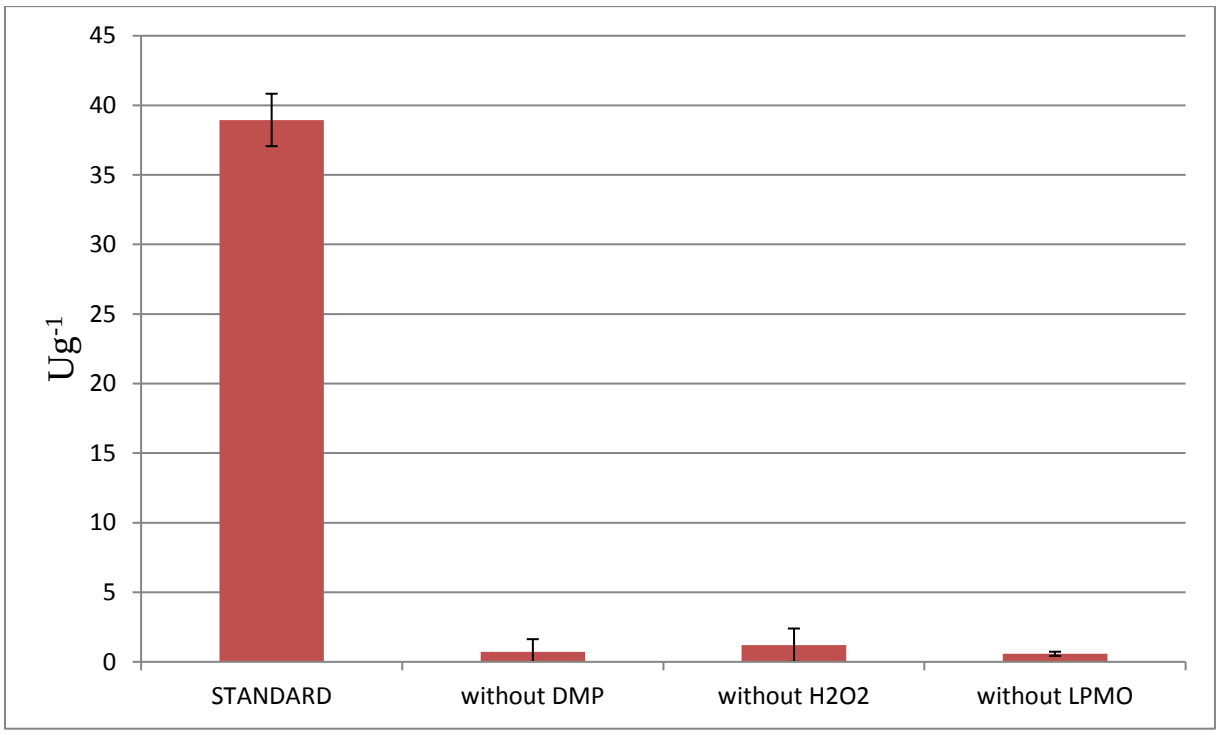

Figure 17. Comparison of specific activities of LPMO using standard assay and assays without: DMP, H_2O_2 and LPMO.

The activity of LPMO in an assay with buffer, DMP, H_2O_2 and enzyme itself amounts 38.95 ± 1.89 Ug^{-1}. Activity in the assay without DMP is 0.72 ± 0.91, without H_2O_2 1.20 ± 1.20 and without LPMO it is 0.58 ± 0.15 Ug^{-1}. Comparing assays without DMP and H_2O_2 with the standard assay, the activity is ~30 times lower, which proves that the substrate and the co-substrate are very important for its activity.

4.2.2. Copper compounds instead of LPMO

As mentioned above, LPMO contains a single copper ion coordinated by the histidine brace in its active side. Using copper compounds instead of LPMO should rule out the possibility that in all those assays LPMO was not the main compound responsible for absorbance shown in spectrophotometric measurements.

Table 4. Results of spectrophotometric measurements of LPMO and copper containing compounds.

	Ug^{-1}
STANDARD (0.5 µM LPMO)	38.95 ± 1.89
$CuSO_4$ 0.5µM with H_2O_2	1.20 ± 0.83
$CuSO_4$ 5µM with H_2O_2	2.94 ± 0.43
$CuSO_4$ 50µM with H_2O_2	16.03 ± 0.56
$CuSO_4$ 0.5µM without H_2O_2	1.47 ± 0.82
$CuSO_4$ 5µM without H_2O_2	2.09 ± 0.89
$CuSO_4$ 50 µM without H_2O_2	5.11 ± 0.77
$CuCl_2$ 0.5µM	1.11 ± 0.15
$CuCl_2$ 5µM	3.23 ± 0.36
$CuCl_2$ 50µM	15.81 ± 0.98

Results represented in Table 4 shows that the highest activity (38.95 ± 1.89 Ug^{-1}) of LPMO is in the standard assay, which contains 0.5 µM LPMO. Comparing to the same concentrations of copper compounds put in the assay instead of LPMO, 0.5 µM $CuSO_4$ shows activity of 1.20 ± 0.83 Ug^{-1} and 0.5µM $CuCl_2$ 1.11 ± 0.15 Ug^{-1}. That is the proof that LPMO is responsible for the reaction that takes action in the cuvette. If the concentrations of these compounds are ten or one hundred times higher (5 and 50 µM), specific activity is proportionally increasing. That is a very important observation when working with LPMO; it is necessary to consider concentrations of copper compounds, if the solution which has to be analyzed contains them. Experiments without hydrogen peroxide were also done and results show that it is not a big difference in activity with and without it if concentrations of copper(II)sulfate are small. When $CuSO_4$ concentration is 50 µM, its activity without peroxide is ~3 times lower than with it (16.03 ± 0.56 to 5.11 ± 0.77 Ug^{-1}). This is a hint to H_2O_2 acting in reactions with copper ions.

4.2.3. Stability assays

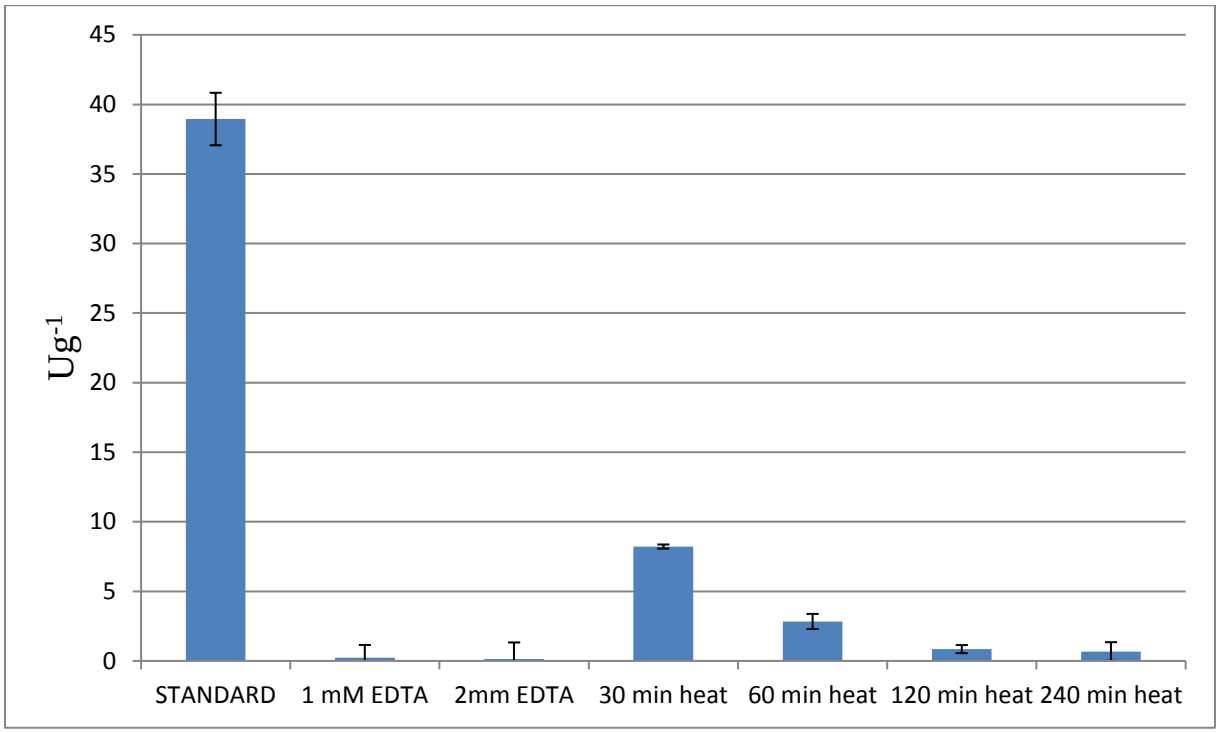

Figure 18. Comparison of specific activities of LPMO in standard assay and assays with LPMO incubating with different EDTA concentrations and LPMO exposure to high temperature during different time intervals.

Results in diagram above show that already 1 mM EDTA is high enough to inactivate LPMO. The activity decreased from 38.95 ± 1.89 Ug^{-1} to 0.24 ± 0.54 Ug^{-1}. Since EDTA is used for scavenging metal ions which deactivate metal-dependent enzymes, these results are expected because of the copper ion in the active side of LPMOs. From the results of the heat test it is visible that LPMO is affected by high temperatures. The longer it is exposed to ~100°C, activity is less. After 30 minutes, LPMOs activity is decreased ~5 times (from 38.95 ± 1.89 Ug^{-1} to 8.22 ± 0.67 Ug^{-1}) and after 240 minutes (4 hours) activity is about 57 times lower (38.95 ± 1.89 Ug^{-1} to 0.68 ± 1.53 Ug^{-1}). Furthermore we have to note that the LPMO solution (1 mL, stored on ice) was incubated in an eppendorf tube in a heat block and that it took time to heat the sample up.

4.3. pH PROFILE

4.3.1. Anionic buffers

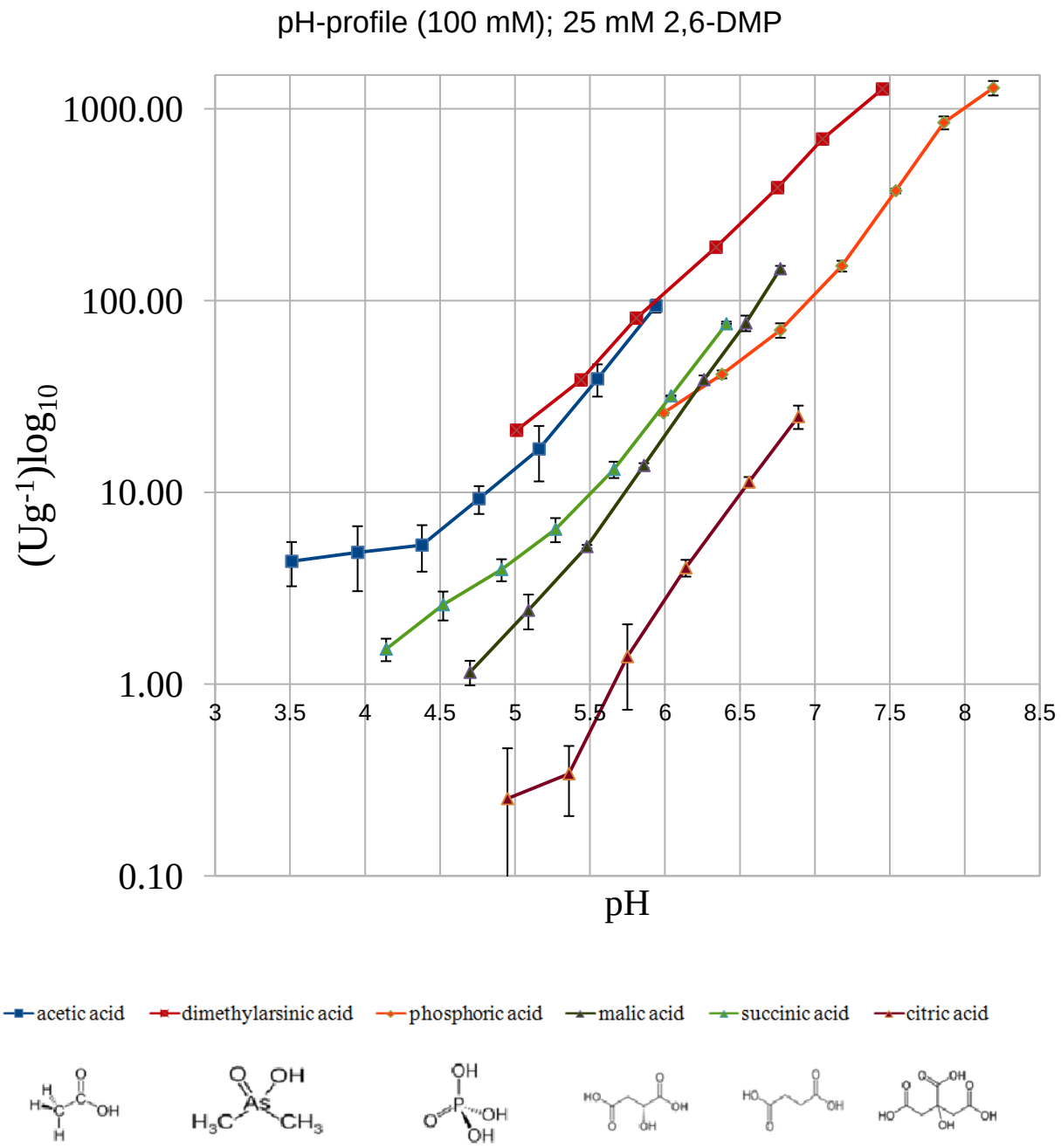

Figure 19. Specific activity of LPMO depending on the different anionic buffers (and their chemical structures) at different pH values.

From the results shown in Figure 19, it is clear that LPMO activity is increasing together with the increase of pH. Acetic acid, succinic acid, malic acid and citric acid buffers have similiar slopes, however, the overall activity is decreasing. According to the chemical structures of these acids, it can be concluded that LPMO activity is higher in buffers with less carboxylic groups and hydroxylic groups. Dimethylarsinic acid and phosphoric acid buffers are, according to the graph, the best anionic buffers for LPMO assays. Its activity can be detected in the pH range from 5.0 to 8.19 and it is 1284.5 ± 111.7 Ug^{-1} for phosphoric acid and 1266.4 ± 40.4 Ug^{-1} for dimethylarsinic acid. Comparing to the buffers mentioned above, the highest LPMO activity was measured in malic acid buffer at pH 6.77 and it is 146.6 ± 5.0 Ug^{-1} which is ~8.8 and ~ 8.6 times lower than phosphoric acid buffer and dimethylarsinic acid buffer, respectively. For dimethylarsinic acid and phosphoric acid, a similar effect as for the other buffers regarding increasing activity with less hydroxyl groups can be observed.

4.3.2. Kationic buffers

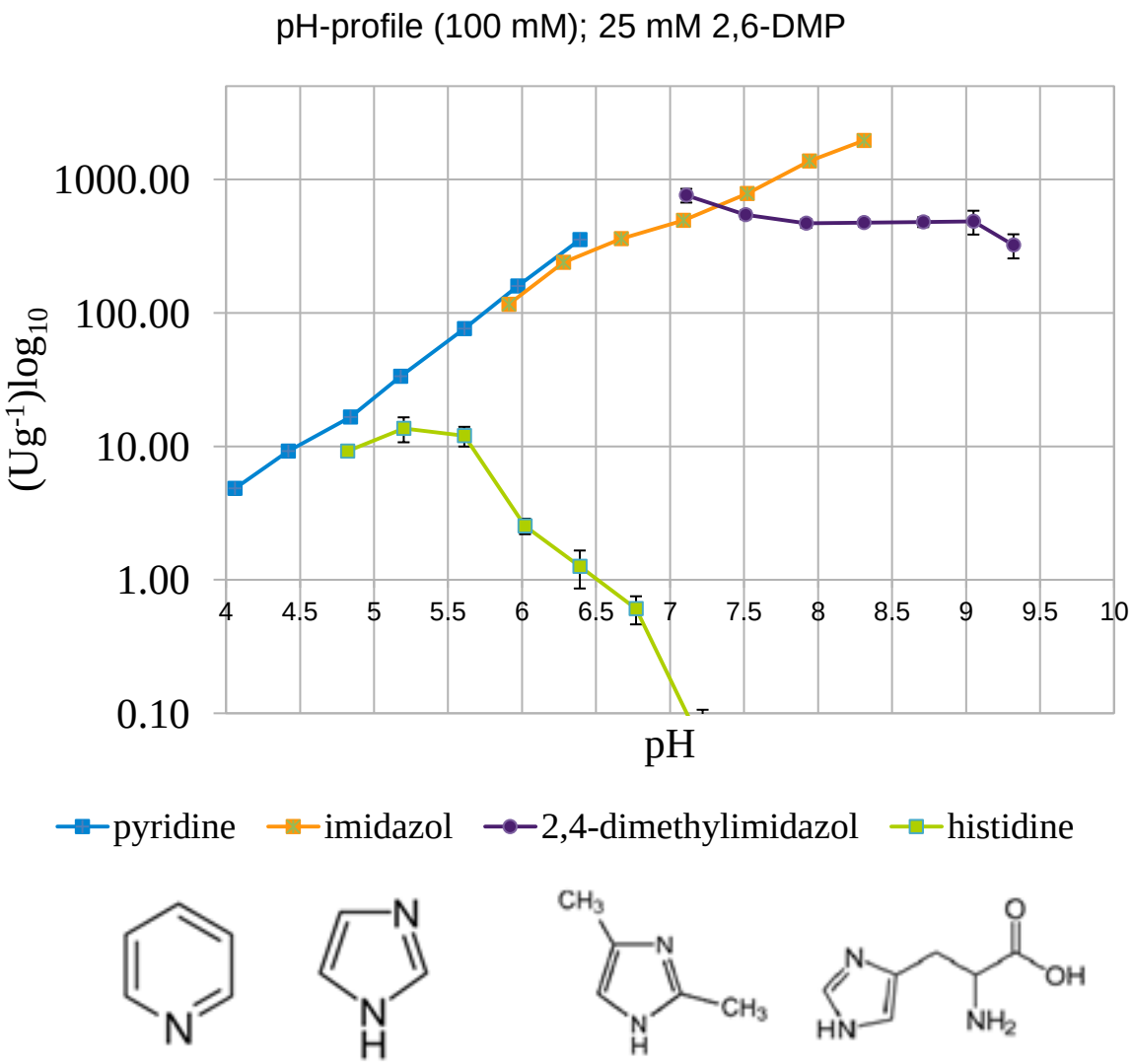

Figure 20. Specific activity of LPMO depending on the different kationic buffers (and their chemical structures) at different pH values.

As it is visible from the results in Figure 20, histidine is bad buffer for LPMO activity assays, because the activity drops to more or less zero with neutral pH. When using 2,4-dimethylimidazol buffer, activity is decreasing with the higher pH values (from ~7-8), then it becomes constant (at pH 7.92 LPMO activity is 468.6 ± 35.0 Ug^{-1}, at pH 8.31 it is 473.5 ± 29.8 Ug^{-1}, at pH 8.71 it is 479.8 ± 40.3 Ug^{-1} and at pH 9.05 it amounts 484.4 ± 98.4 Ug^{-1}) and after pH ~9.0 it starts decreasing again. No further experiments were done in order to explain these results. In the case of histidine, presumption is that these results can be somehow related

to „histidine brace“ in the active site of LPMO and that the buffer species is strongly binding in the more deprotonated state.

Pyridine and imidazol buffers are convenient for doing LPMO assays, each of them in different pH range, which is shown through increase of activity by increasing the pH values. LPMO shows linear increasing in activity in Pyridine buffer from pH 4.06 to 6.39 at which it is the highest and amounts 353.1 ± 23.1 Ug^{-1}. Since imidazol has higher pKa value (7.05) than pyridine (5.24), it was possible to conduct the experiments at higher pH values. In Imidazol buffer, activity is also rising from pH 5.91 to 8.31 but it becomes linear around pH 7. The highest activity is at the highest pH and it amounts 1956.5 ± 84.9 Ug^{-1}.

4.3.3. Buffer combinations

From the results presented and explained in Figure 19 and Figure 20, the best combination of buffer species can be created using succinic acid and phosphoric acid, because it is clearly shown in Figure 19 that enzyme activity in phosphoric acid buffer actually continues to activity in succinic acid buffer which was measured at lower pH values because of the lower pKa value (7.21 compared to 5.24). The same situation can be observed in the case of kationic buffers with pyridine and imidazol shown in Figure 20. LPMO activity in imidazol buffer continues to pyridine buffer where it was measured at lower pH because of the same reason already mentioned above (pKa values). Because of these results, succinic-phosphoric buffer and pyridine-imidazol buffer were made and specific activity was measured. Results are shown in the graph below.

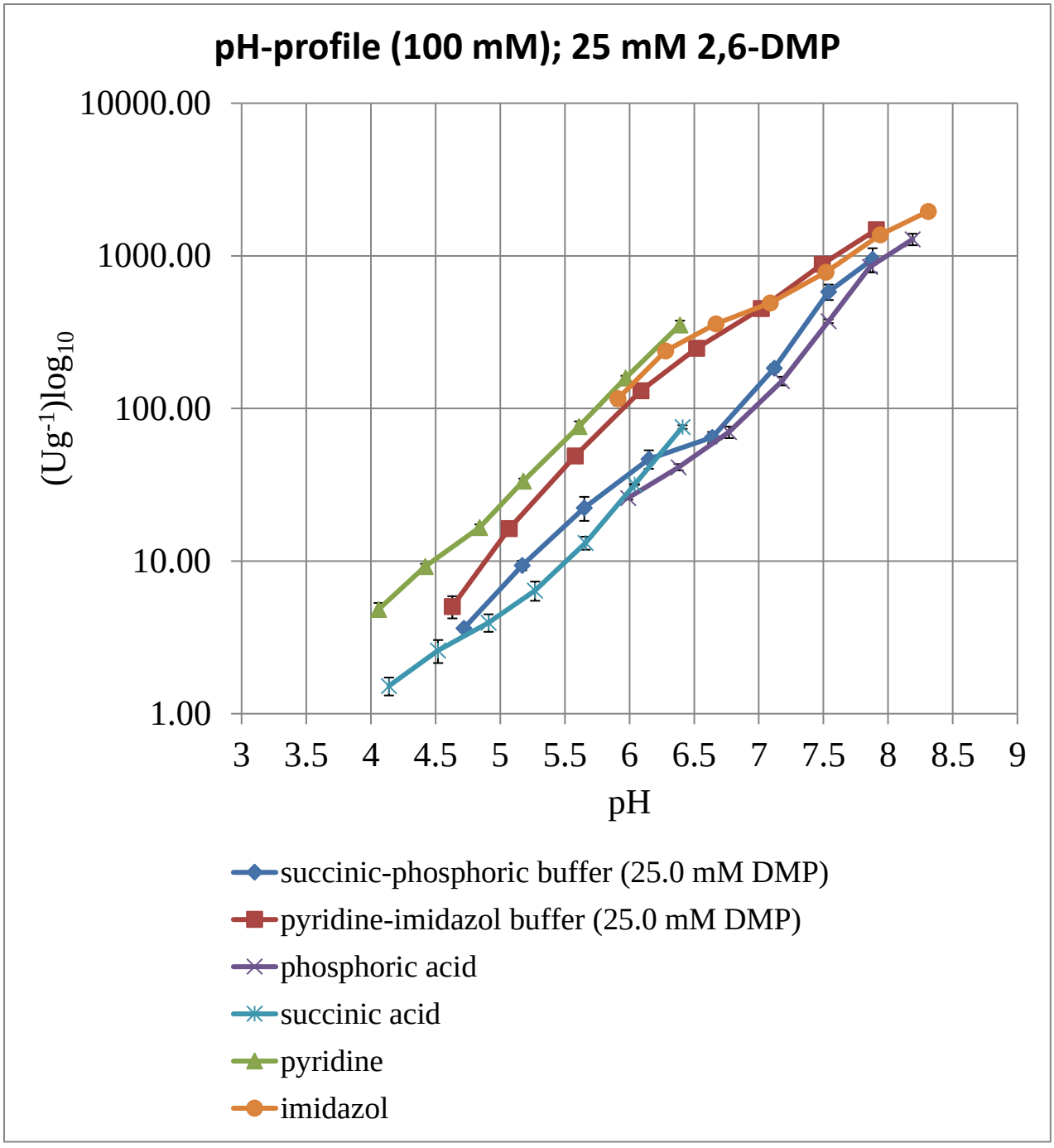

Figure 21. Results from measuring activity in succinic-phosphoric buffer and pyridine-imidazol buffer and in their individual compounds.

LPMO activity is very similar in both combinations. There are very small differences, which are caused by measuring errors or preparation, however, it is clearly seen in the Figure 21 that both succinic-phosphoric buffer and pyridine-imidazol buffer are very convenient and should be used in LPMO activity assays, especially because they encompass a very large range of pH values, from 4.72 to 7.88 and 4.63 to 7.91, respectively.

4.4. TEMPERATURE EFFECT ON LPMO

Proteins can be denaturated by heat, as it was proven for LPMO in Figure 18. If the temperature is increasing slowly, protein conformation remains intact until it quickly loses its structure and function in the narrow temperature range (Nelson and Cox, 2012).

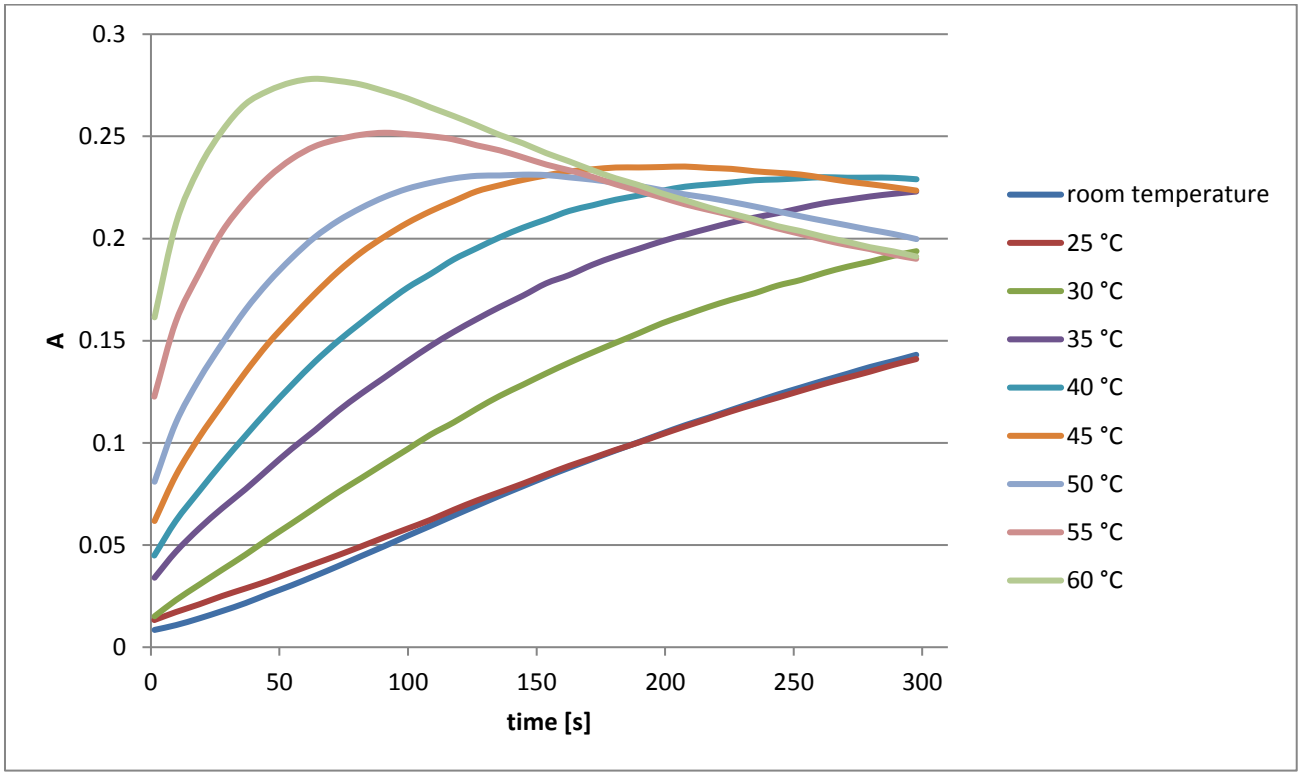

Figure 22. Correlation between absorption rates during time for LPMO incubated at different temperatures.

Since absorption is proportional to enzyme activity, it is obvious that LPMO activity is lost faster at higher temperature. In Figure 22 it is shown that in a temperature range from room temperature to around 35°C the slope is linear, which means activity is not lost during 300 s. Around 40°C, after ~200 s there is no slope anymore, just a straight line, and in a range from 45°C to, in this case, 60°C, slope reaches negative values. The plateau and following decrease in absorption can be explained by totally inactivated LPMO. We guess that inactivation at lower temperature occurs from the reaction mechanism with H_2O_2 rather than from the temperature, because at this low temperatures (e.g. 40°C) the enzyme should be stable. At higher temperatures (e.g. 60°C) we hypothesize that both, a mixture of heat inactivation and inactivation due to H_2O_2, are the reasons for the early end of activity. Nevertheless, the activation energy of the enzyme reaction was calculated through Arrhenius

equation ($k = A * e^{(-Ea/RT)}$) from the linear range. Expressed in natural logarithmic form ($\ln k = \ln A - (E_a/R*1/T)$), the Arrhenius equation allows calculation of E_a (activation energy) by plotting ln (natural logarithm) of the initial rate of the reaction on y axis vs. 1/T (temperature in Kelvin) on x axis. The slope is equal to $-E_a*R$.

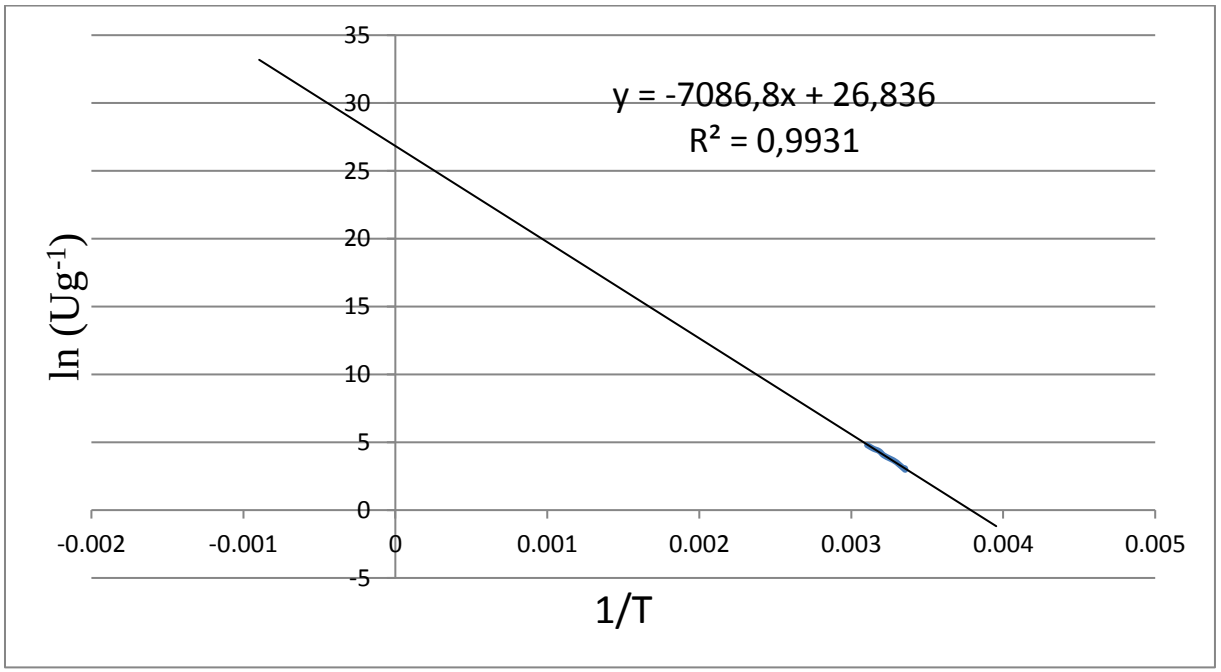

Figure 23. Results in calculation of trendline by plotting logarithmic values of the initial rate of reactions versus reciprocal value of temperature in Kelvin.

From the calculated slope, linear regression; y = - 7086.8x + 26.836, E_a was calculated (Figure 23). Since -7086.8 correspond to $-E_a*R$ and R is a gas constant which amounts 8,314 $Jmol^{-1}K^{-1}$, E_a was calculated by multiplying -7086.8 with 8.314 and -1 to get the positive E_a value. Result is 58.92 $kJmol^{-1}$. This is the amount of energy that is required to overcome the activation barrier which represents the transition state that must be overcome in the conversion of reactants into products (Nelson and Cox, 2012).

4.5. LPMO KINETICS

4.5.1. K_M and V_{max} values measured for H_2O_2

Table 5. V_{max} and K_M values of LPMO for H_2O_2 calculated for different DMP concentrations measured in succinic-phosphoric buffer at pH 6.0.

DMP [mM]	**V_{max} [Ug^{-1}]**	**K_M [µM]**
0.5	2.00 ± 0.08	5.89 ± 1.36
1	3.99 ± 0.23	8.80 ± 2.70
2	9.21 ± 0.46	20.10 ± 5.03
10	32.62 ± 0.72	23.32 ± 2.49
25	58.73 ± 1.37	24.11 ± 2.72
50	104.66 ± 3.61	24.63 ± 4.11
85	126.52 ± 6.43	16.99 ± 4.40
115	153.95 ± 7.63	6.29 ± 1.71

Table 6. V_{max} and K_M values of LPMO for H_2O_2 calculated for different DMP concentrations measured in succinic-phosphoric buffer at pH 7.0.

DMP [mM]	**V_{max} [Ug^{-1}]**	**K_M [µM]**
0.5	17.38 ± 0.59	2.18 ± 0.47
1	28.75 ± 0.61	2.20 ± 0.29
2	45.64 ± 0.94	2.30 ± 0.30
10	151.52 ± 5.59	1.95 ± 0.47
25	257.09 ± 7.34	1.90 ± 0.36
50	543.07 ± 19.01	1.08 ± 0.31
85	809.35 ± 27.37	0.40 ± 0.20
115	865.52 ± 24.71	0.38 ± 0.17

Results shown in Table 5 and 6 again prove that LPMO is more active at higher pH values. At pH 6.0, LPMO reaches 2.00 ± 0.08 Ug^{-1} and at pH 7.0 it reaches 17.38 ± 0.59 Ug^{-1}, measured with the same DMP concentration (0.5 mM). That is ~9 times higher maximum velocity. When observing the highest DMP concentration used (115 mM), Vmax is also different for pH 6.0 (153.95 ± 7.63 Ug^{-1}) than for pH 7 (865.52 ± 24.71 Ug^{-1}), leading to the increase of ~7 times. However, when DMP concentration used in assay is increasing, V_{max} are also raising in both pH 6.0 and pH 7.0 measurements. Calculations of K_M are showing different results. As it is expected, K_M values are lower at pH 7.0. In comparison, K_M value measured while using 0.5 mM DMP amounts 5.89 ± 1.36 µM at pH 6.0 and 2.18 ± 0.47 µM at pH 7.0, which is ~3 times lower at higher pH. The thing that is not expected is that with higher DMP concentrations after 50 mM (at pH 6.0) K_M values are decreasing. It started between 25 mM DMP and 50 mM DMP where K_M values are very similar (24.11 ± 2.72 µM and 24.63 ± 4.11 µM, respectively). After 50 mM they are much lower, reaching 6.29 ± 1.71 µM at 115 mM, the value similar to 0.5 mM DMP (5.89 ± 1.36 µM). The decreasing K_M values with high DMP concentrations can be explained due to problems with solubility of the substrate and in general problems with the reaction mechanism caused by the high concentration.

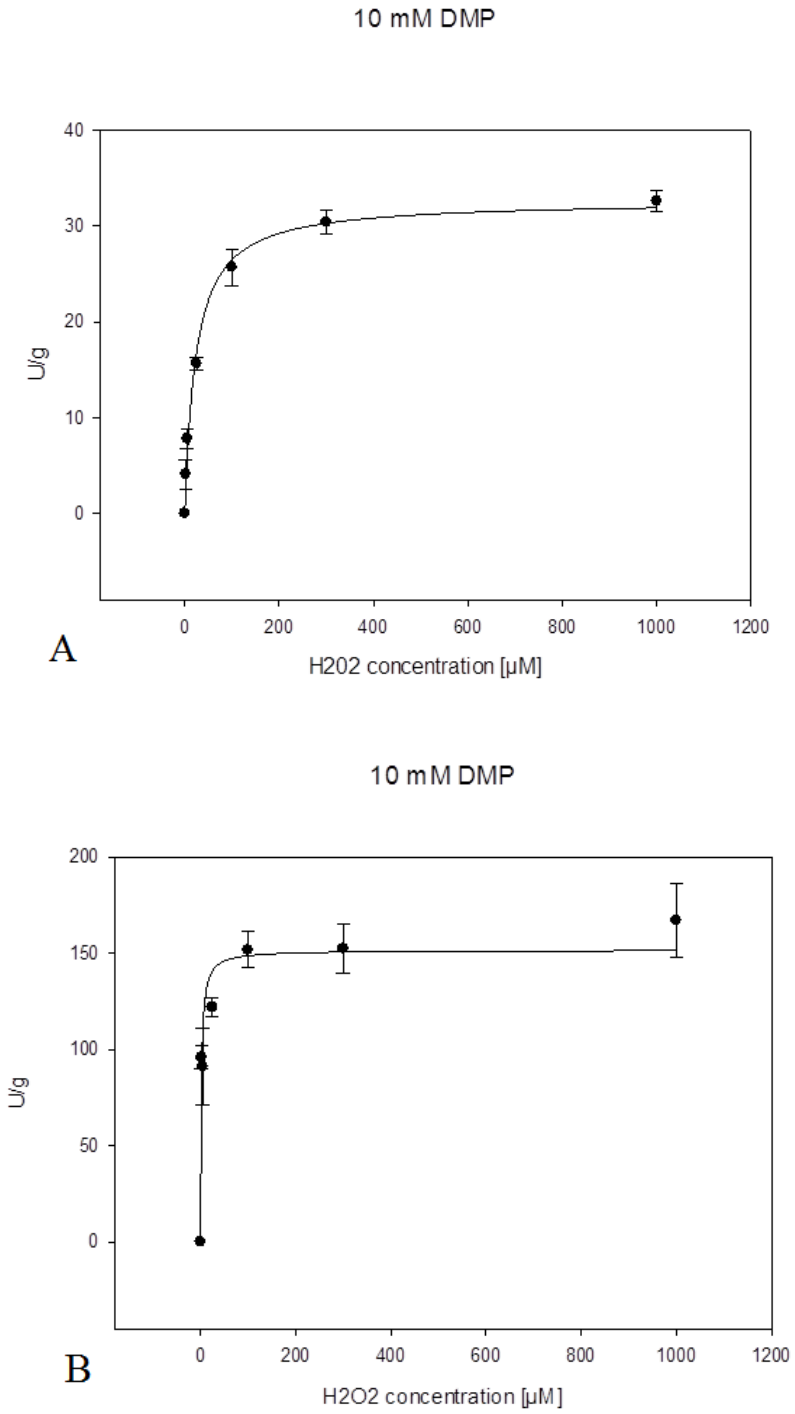

Figure 24. Michaelis-Menten curve for H_2O_2 as a co-substrate for LPMO with 10 mM DMP in the succinic-phosphoric buffer at: A) pH 6.0 and B) pH 7.0.

Michaelis-Menten curves for all DMP concentrations are made and results of K_M and V_{max} values are shown in Table 5 and 6. There are two representative curves shown in Figure 24 where the difference in range of LPMO activity between pH 6.0 and pH 7.0 is clearly visible. Both curves are hyperbolas, which lead to conclusion that H_2O_2 is good co-substrate for LPMO.

4.5.2. K_M and V_{max} values measured for DMP

Table 7. V_{max} and K_M values of LPMO for DMP calculated for different H_2O_2 concentrations measured in succinic-phosphoric buffer at pH 6.0.

H_20_2 [µM]	**V_{max} [Ug^{-1}]**	**K_M [mM]**
2	n.c.	n.c.
5	n.c.	n.c.
25	276.83 ± 4.46	245.44 ± 74.71
100	223.77 ± 16.06	96.82 ± 12.56
300	352.79 ± 43.58	144.75 ± 28.16
1000	314.11 ± 13.73	97.66 ± 7.69

n.c. … not calculated because Michaelis plot showed linear increase in activity

Table 8. V_{max} and K_M values of LPMO for DMP calculated for different H_2O_2 concentrations measured in succinic-phosphoric buffer at pH 7.0.

H202 [µM]	**Vmax [Ug^{-1}]**	**Km [mM]**
2	3884.29 ± 1844.12	420.78 ± 243.08
5	2269.89 ± 553.11	249.79 ± 82.35
25	2124.74 ± 405.97	171.91 ± 49.09
100	1921.55 ± 289.39	131.79 ± 32.22
300	1923.92 ± 293.28	123.96 ± 31.31
1000	2165.94 ± 229.50	140.47 ± 23.67

In the experiments where H_2O_2 was kept constant and DMP concentrations were different (Table 7 and 8), the same thing occurred as in the experiments explained in 4.5.1. V_{max} values are higher at higher pH (pH 7.0), when comparing the same H_2O_2 concentrations (for example, V_{max} is ~8.5 times higher at pH 7.0 for 100 μM H_2O_2). The same thing does not occur for K_M (values are not lower at higher pH as in previous case). For 100 μM H_2O_2, K_M at pH 6.0 is lower (96.82 ± 12.56 mM) than at pH 7.0 (131.79 ± 32.22 mM). Interestingly, at pH 6.0, when using 2 and 5 μM hydrogen peroxide, values could not be calculated because trends are linear (Figure 25), so there is no Michaelis-Menten hyperbolic curve. For the same concentrations at pH 7.0, V_{max} and K_M values are calculated because trend is not as linear as at pH 6.0 (Figure 26), but values are very high and predicted and standard deviations are really big. V_{max} and K_M values for 2 μM H_2O_2 are 3884.29 ± 1844.12 Ug^{-1} and 420.78 ± 243.08 mM, respectively and for 5 μM H_2O_2 maximal activity amounts 2269.89 ± 553.11 Ug^{-1} and K_M is 249.79 ± 82.35 mM. These values of DMP can not be reached in LPMO activity assays because its solubility is much lower. It is also unexpected that there is no increasing of V_{max} values, i.e. decreasing of K_M values as H_2O_2 concentrations are higher. For example, at pH 6.0, V_{max} in the assay with 25 μM H_2O_2 is 276.83 ± 4.46 Ug^{-1}, then with 100 μM H_2O_2 it goes down and amounts 223.77 ± 16.06 Ug^{-1} to get 352.79 ± 43.58 Ug^{-1} with 300 μM H_2O_2. The same thing is happening with the K_M (245.44 ± 74.71 mM, 96.82 ± 12.56 mM and 144.75 ± 28.16 mM, respectively).

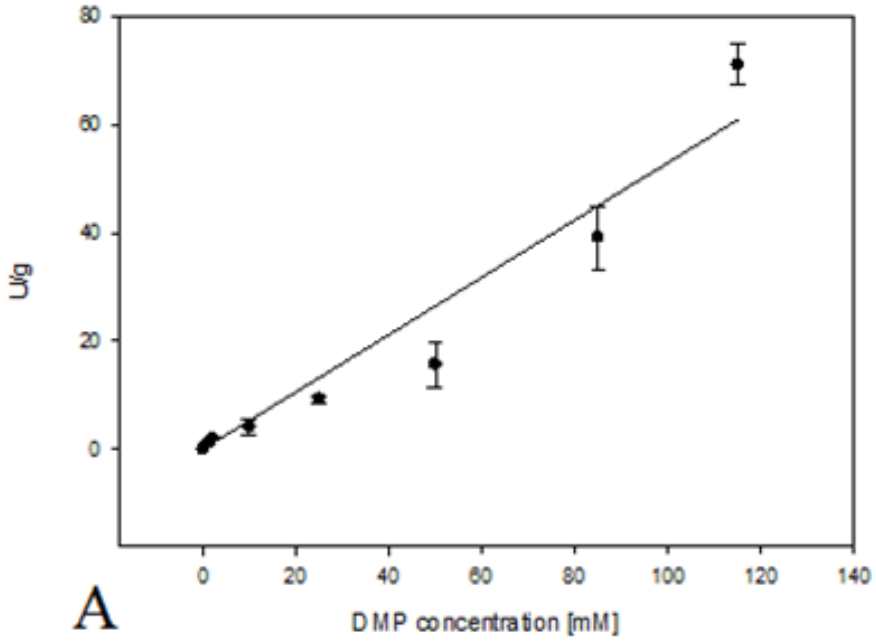

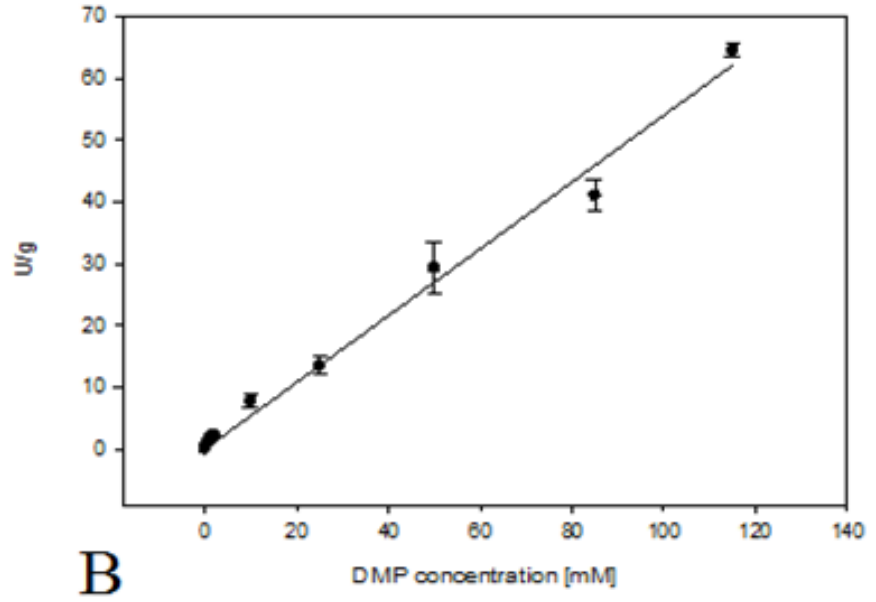

Figure 25. Results for LPMO activity for different DMP concentrations spectrophotometricaly measured in succinic-phosphoric buffer at pH 6.0 with A) 2 μM H_2O_2 and B) 5 μM H_2O_2.

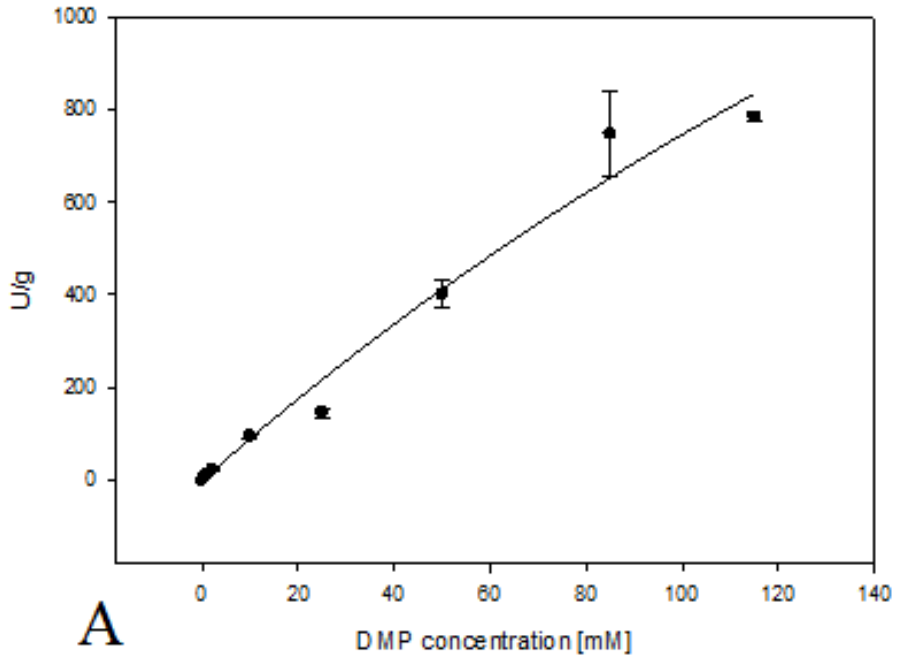

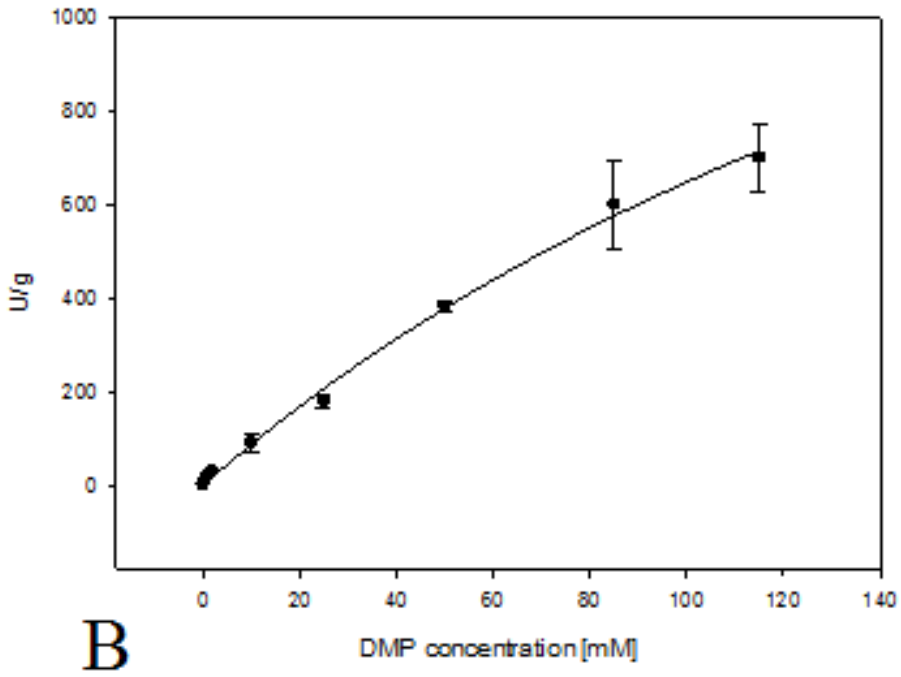

Figure 26. Results for LPMO activity for different DMP concentrations spectrophotometricaly measured in succinic-phosphoric buffer at pH 7.0 with A) 2 μM H_2O_2 and B) 5 μM H_2O_2.

4.6. LIMIT OF DETECTION (LoD)

Table 9. Results of spectrophotometricaly measured specific activity of different LPMO concentrations.

Dilutions	**LPMO concentration [μM]**	**Ug^{-1}**
D0 = original sample	10	18.41 ± 0.86
D2 = 2x diluted	5	13.12 ± 0.75
D4 = 4x diluted	2.5	8.43 ± 0.14
D8 = 8x diluted	1.25	4.83 ± 0.04
D10 = 10x diluted	1	3.93 ± 0.34
D20 = 20x diluted	0.5	1.95 ± 0.09
D40 = 40x diluted	0.25	1.02 ± 0.04
D80 = 80x diluted	0.125	0.58 ± 0.03
D100 = 100x diluted	0.1	0.42 ± 0.05
D200 = 200x diluted	0.05	0.24 ± 0.01
D400 = 400x diluted	0.025	0.10 ± 0.02
D800 = 800x diluted	0.0125	0.06 ± 0.02

Since the original sample is 10 μM LPMO and its specific activity is 18.41 ± 0.86 Ug^{-1}, it is expected that all the other solutions would have as lower activity as they are diluted. That is not exactly the case. 5 μM LPMO shows specific activity of 13.12 ± 0.75 Ug^{-1} which is ~1.4 and not two times lower then the activity of the original sample. 2.5 μM LPMO has the activity of 8.43 ± 0.14 Ug^{-1}, which is ~2 times lower than 10 μM LPMO and ~1.5 lower than 5 μM LPMO. Eight times diluted LPMO (1.25 μM) is 4.83 ± 0.04 Ug^{-1}which is ~3.8 times lower than the activity of non diluted LPMO (18.41 ± 0.86 Ug^{-1}) and not 8 times as it is expected. The same is when comparing to D2 or D4. D10 is ten times diluted LPMO (1 μM) and comparing to D0, it has ~4.7 lower activity (3.93 ± 0.34 Ug^{-1} to 18.41 ± 0.86 Ug^{-1}). On the other hand, dilutions made from D10 are D20, D40 and D80 and has ~2, ~3.9 and ~6.8 times less activity, respectively. These results are good ovarlepping with expectations. 0.1 μM LPMO (D100) should have one hundred times lower activity than 10 μM LPMO, but

experiments show ~44 times. Dilutions made from D100 are D200, D400 and D800 and they has 1.75, 4.2 and 7 times lower activities, respectively.

These results from Table 9 leads to the conclusion that higher concentrations of LPMO are not following regularity of the dilutions as lower concentrations. In Figure 27 it is visible that above some concentration, LPMOs activity is starting leveling of.

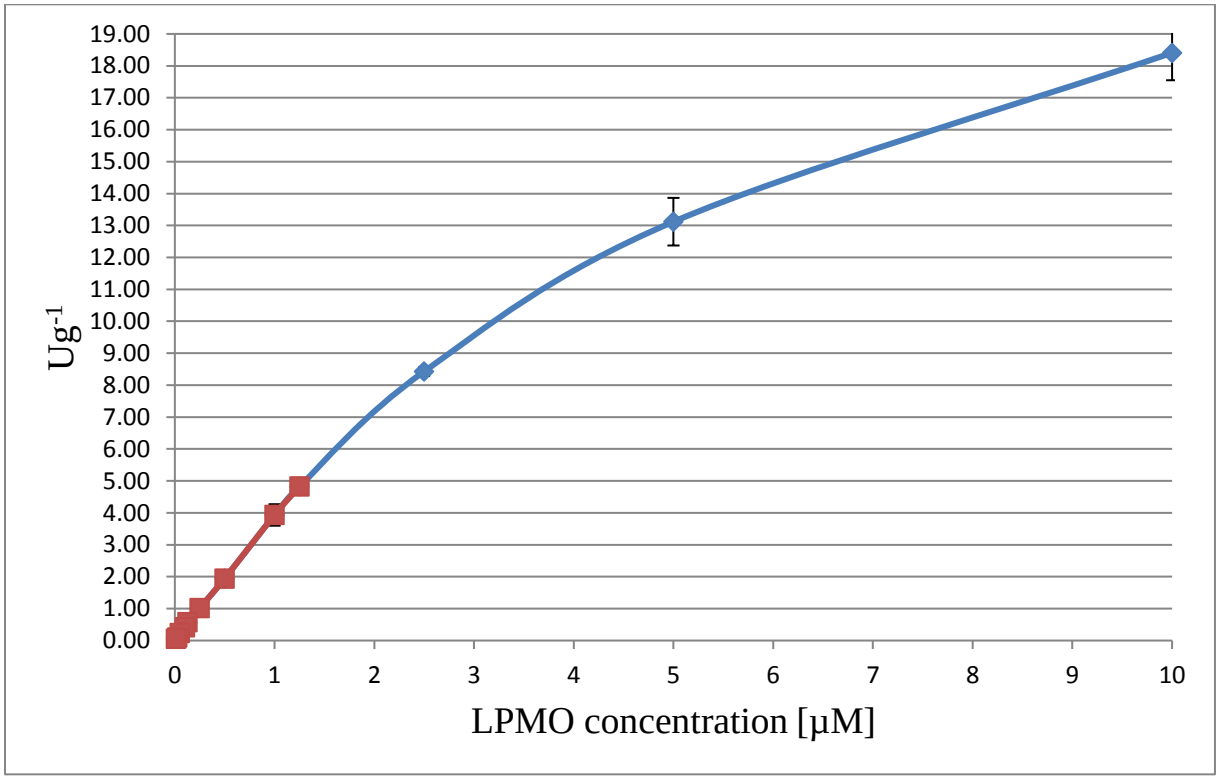

Figure 27. Correlation beetween specific activity [Ug^{-1}] and LPMO concentration [µM].

As mentioned above, after 1.25 µM LPMO the slope is leveling of. It is also interesting that standard deviations are larger in this case, so assays this way should not be done at higher LPMO concentration because the linear slope will not appear and the results will be hard to determine.

The main purpose of this experiment was to determine LoD, i.e. the lowest LPMO concentration which will produce a signal greater and can reliably be distinguished from the analytical noise. It is calculated that standard deviation of blanks amounts $9.29 * 10^{-7}$ AU (Apsorbance units) and standard deviation of absorbance measured for the lowest LPMO concentration (0.0125 µM) is $5.55 * 10^{-6}$ AU which is ~18 times higher. Since, in theory, standard deviation of the lowest analyte concentration should be at least three times higher than the blank, conclusion is that 0.0125 µM LPMO is enough to do activity assay in these

conditions. This concentration is the lowest to definitely detect LPMO activity, however, the signal is very low and should only show in which range activity can be detected. For measurements,the concentration of LPMO around 0.5 µM should be used.

5. CONCLUSIONS

1. In order to establish an activity assay for LPMO without using its natural substrate, DMP manifested as the one compound that shows the best properties (spectra is not affected by any other components of the assay) for detecting LPMO activity. In the absence of H_2O_2 activity is much lower, which means that hydrogen peroxide plays an important role as the LPMO co-substrate. On the other hand, it must be added responsibly due to the inhibition effect at too high concentrations. The best buffers for the assay are combinations of succinic and phosphoric acid buffer and pyridine and imidazol buffer. Activity can be determined in a very wide range of pH values (from ~4.5 to ~8.0).
2. Because of the copper ion in its active site, LPMO can not withstand high concentrations of EDTA. The same effect is with heat. After 30 minutes at ~100°C LPMO activity is lower about five times. What has to be considered when working with LPMO is concentration of compounds with copper in the solution because it is proven that their activity is increasing with concentration and LPMO activity can be interpreted wrong if this is a case.
3. The activation energy for LPMO is 58.92 $kJmol^{-1}$. This is the amount of energy that is required to overcome the activation barrier in the conversion of reactants into products.
4. According to results in calculations of K_M and V_{max} values, it is one more time proven that hydrogen peroxide is a good co-substrate for LPMO. On the other hand, DMP is not showing Michaelis-Menten curve, but it is linear as in non-catalyzed reactions, which leads to conclusion it is not a natural substrate for LPMO.
5. The highest LPMO concentration that should be used in activity assay is ~1.25 μM because all the tested concentrations above show deviation from linearity. Contrary, the lowest LPMO concentration that can be used in assay is ~0.0125 μM.

6. REFERENCES

Aachmann, F. L., Sørlie, M., Skjåk-Bræk, G., Eijsink, V. G. H., Vaaje - Kolstad, G. (2012) NMR structure of a lytic polysaccharide monooxygenase provides insight into copper binding, protein dynamics, and substrate interactions. *PNAS* **109** (46), 18779 - 18784.

Adelakun, O. E., Kudanga, T., Green, I. R., Roes - Hill, M., Burton, S. G. (2012) Enzymatic modification of 2,6 - Dimethoxyphenol for the synthesis of dimers with high antioxidant capacity. *Process Biochem.* **47**, 1923 - 1932.

Agger, J. W., Isaksen, T., Várnai, A., Vidal - Melgosa, S., Willats, W. G. T., Ludwig, R., Armbruster, D. A., Pry, T. (2008) Limit of Blank, Limit of Detection and Limit of Quantitation. *Clin. Biochem.* **29**, 49-52.

Beeson, W. T., Philips, C. M., Cate, J. H. D., Marletta, M. A. (2011) Oxidative Cleavage of Cellulose by Fungal Copper-Dependent Polysaccharide Monooxygenases. *J. Am. Chem. Soc.* **134**, 890-892.

Bissaro, B., Røhr, Å., Müller, G., Chylenski, P., Skaugen, M., Forsberg, Z., Horn, S. J., Vaaje - Kolstad, G., Eijsink, V. G. H. (2017) Oxidative cleavage of polysaccharides by monocopper enzymes depends on H_2O_2. *Nat. Chem. Biol.* **13**, 1123 - 1128.

Bissaro, B., Røhr, Å., Skaugen, M., Forsberg, Z., Horn, S. J., Vaaje - Kolstad, G., Eijsink, V. G. H. (2016) Fenton-type chemistry by a copper enzyme: molecular mechanism of polysaccharide oxidative cleavage. *bioR$_x$iv beta: The preprint server for biology.* doi: https://doi.org/10.1101/097022

Borisova, A. S., Isaksen, T., Dimarogona, M., Kognole, A. A., Mathiesen, G., Várnai, A., Røhr, Å. K., Payne, C. M., Sørlie, M., Sandgren, M., Eijsink, V. G. H. (2015) Structural and Functional Characterization of a Lytic Polysaccharide Monooxygenase with Broad Substrate Specificity. *J. Biol. Chem.* **290** (38), 22955 - 22969.

Burns, R. G., Dick, R. P. (2002) *Enzymes in the Environment: Activity, Ecology and Application*, Marcel Dekker, Inc., New York.

CAZy (2017) CAZy - Carbohydrate Active Enzyme, < http://www.cazy.org/> . Accesed 5 October 2017

Chen, H. (2014) *Biotechnology of lignocelluloses: Theory and practice,* Springer Science + Bussines Media B.V., Dordrecht. doi: 10.1007/978-94-007-6898-7

Dimarogona, M., Topakas, E., Christakopoulos, P. (2012) Cellulose degradation by oxidative enzymes. *Computat. Struct. Biotechnol. J.l* **2** (3), e201209015.

Dimarogona, M., Topakas, E., Christakopoulos, P. (2013) Recalcitrant polysaccharide degradation by novel oxydative biocatalysts. *Appl. Microbiol. Biotechnol.* **97**, 8455 - 8465. doi: 10.1007/s00253-013-5197-y

Forsberg, Z., Vaje - Kolstad, G., Westereng, B., Zarah Forsberg, Gustav Vaaje-Kolstad, Bjørge Westereng, Bunæs, A.,C., Stenstrøm, Y., MacKenzie, A., Sørlie, M., Horn, S. J., Eijsink, V. G., H. (2011) Cleavage of cellulose by a CBM33 protein. *Protein Sci.* **20**, 1479 - 1483. doi: 10.1002/pro.689

Frandsen, K. E. H., Simmons, T. J., Dupree, P., Poulsen, J. - C. N., Hemsworth, G. R., Ciano, L., Johnston, E. M., Tovborg, M., Johansen, K. S., von Freiesleben, P., Marmuse, L., Fort, S., Cottaz, S., Hugues, D., Henrissat, B., Lenfant, N., Tuna, F., Baldansuren, A., Davies, G. J., Leggio, L. L., Walton, P. H. (2016) the molecular basis of polysaccharide cleavage by lytic polysaccharide monooxygenases. *N. Chem. Bio.* **12**, 298 - 303. doi: 10.1038/nchembio.2029

Hemsworth, G. R., Davies, G. J., Walton, P. H. (2013) Recent insights into copper-containing lytic polysaccharide monooxygenases. *Curr. Opin. Struc. Biol.* **23** (5), 660 - 668.

Hemsworth, G. R., Johnston, E. M., Davies, G. J., Walton, P. H. (2015) Lytic Pollysaccharide Monooxygenases in Biomass Conversion. *Trends. Biotechnol.* **33** (12), 747 - 761.

Horn, S. J., Eijsink, V. G. H., Westereng, B. (2014) Discovery of LPMO activity on hemicelluloses shows the importance of oxidative processes in plant cell wall degradation. *PNAS* **111** (7), 6287 - 6292.

Horn, S. J., Vaaje - Kolstad, G., Westereng, B., Eijsink, V. G., H. (2012) Novel enzymes for degradation of cellulose. *Biotechnol. Biofuels*, **5**:45.

Ioelovich, M., Morag, E. (2012) Study of enzymatic hydrolysis of mild pretreated lignocellulosic biomasses. *BioResources* **7** (1), 1040-1052.

Isaksen, T., Westereng, B., Aachman, F. L., Agger, J. W., Kracher, D., Kittl, R., Ludwig, R., Haltrich, D., Eijsink, V. G., H., Horn, S. J. (2014.) A C4 - oxidizing Lytic Polysaccharide

Monooxygenase Cleaving Both Cellulose and Cello - oligosaccharides. *J. Biol. Chem.* **289**, 2632 - 2642.

Johansen, K. S. (2016) Lytic Polysaccharide Monooxygenases: The Microbial Power Tool for Lignocellulose Degradation. *Trends. Plant. Sci.* **21** (11), 926 - 936.

Kittl, R., Kracher, D., Burgstaller, D., Haltrich, D., Ludwig, R. (2012) Production of four Neurospora crassa lytic polysaccharide monooxygenases in Pichia pastoris monitored by a fluorimetric assay. *Biotechnol. Biofuels*, **5**:79.

Kobayashi, H., Fukuoka, A. (2013) Synthesis and utilisation of sugar compounds derived from lignocellulosic biomass. *Green Chem.* **15**, 1740 - 1763. doi: 10.1039/C3GC00060E

Loose, J. S. M., Forsberg, Z., Fraaije, M. W., Eijsink, V. G. H., Vaaje - Kolstad, G. (2014) A rapid quantitative activity assay shows that the *Vibrio cholera* colonization factor *GbpA* is an active lytic polysaccharide monooxygenase. *FEBS Lett.* **588**, 3435-3440. doi: 10.1016/j.febslet.2014.07.036

Nelson, D. L., Cox, M. M. (2012) *Lehninger Principles of Biochemistry*, 6th ed., W. H. Freeman, & Company, New York.

PDB (2017) An Information Portal to 134091 Biological Macromolecula Structure, PDB - Protein Data Bank, < http://www.rcsb.org>. Accesed 9 October 2017.

Philips, C. M., Beeson, W. T., Cate, J. H., Marletta, M. A. (2011) Cellobiose Dehydrogenase and a Copper-Dependent Polysaccharide Monooxygenase Potentiate Cellulose Degradation by Neurospora crassa. *ACS Chem. Biol.* **6**, 1399 - 1406.

Rinaudo, M. (2006) Chitin and chitosan: Properties and applications. *Prog. Polym. Sci.* **31** (7), 603 - 632.

Sluiter, J. B., Ruiz, R. O., Scarlata, C. J., Sluiter, A. D., Templeton, D. W. (2010) Compositional analysis of lignocellulosic feedstocks, 1. Review and description of methods, *J. Agric. Food Chem.* **58**, 9043–9053.

Span, E. A., Marletta, M. A. (2015) The framework of polysaccharide monooxygenase structure and chemistry. *Curr. Opin. Struc. Biol.* **35**, 93-99.

Vaaje - Kolstad, G., Forsberg., Z., Loose, Jenifer, S. M., Bissaro, B., Eijsink, V. G. H. (2017) Structural diversity of lytic polysaccharide monooxygenases. *Curr. Opin. Struc. Biol.* **44**, 67 - 76.

Wariishi, H., Valli, K., Gold, M. H. (1992) Manganese(I1) Oxidation by Manganese Peroxidase from the Basidiomycete *Phanerochaete chrysosporium. J. Biol. Chem.* **267** (33), 23689-23695.

7. APPENDIX

7.1. K_M AND V_{max} VALUES MEASURED FOR H_2O_2 IN SUCCINIC-PHOSPHORIC BUFFER AT pH 7.5

Table 10. K_M and V_{max} values of LPMO for H_2O_2 calculated for different DMP concentrations measured in succinic-phosphoric buffer at pH 7.5.

DMP [mM]	**V_{max} [Ug^{-1}]**	**K_M [μM]**
0.5	20.11 ± 0.84	5.39 ± 1.16
1	34.88 ± 0.85	10.69 ± 1.13

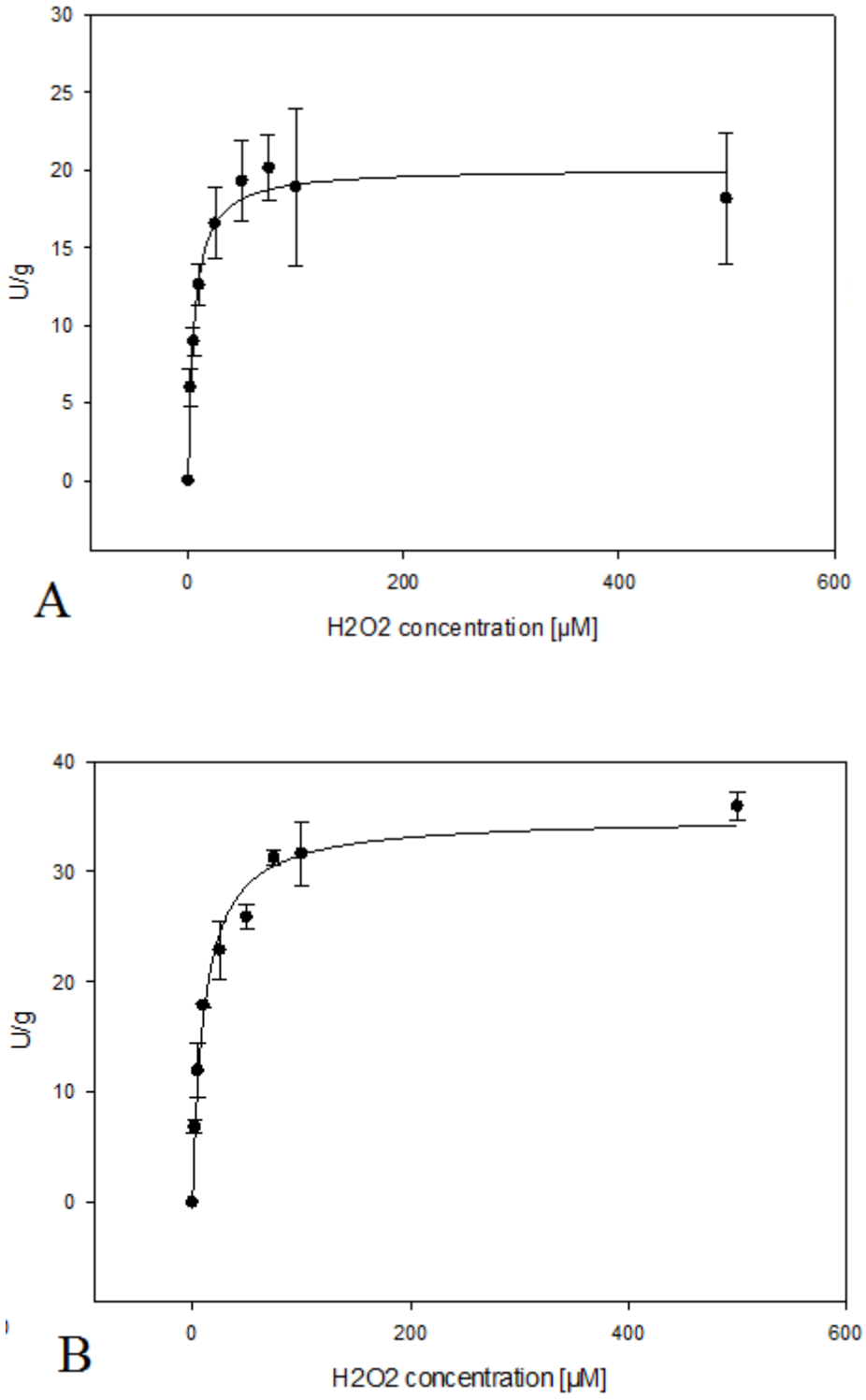

Figure 28. Michaelis-Menten curve for H_2O_2 as a co-substrate for LPMO in the succinic-phosphoric buffer at pH 7.5 with: A) 0.5 mM DMP and B) 1 mM DMP.

7.2. LIST OF ABBREVIATIONS

AA	Auxiliary activities
AU	Apsorbance units
CBM	Carbohydrate-binding module
CDH	Cellobiose dehydrogenase
DMP	2,6-dimethoxyphenol
EDTA	Ethylenediaminetetraacetic acid
GH	Glycoside hydrolase
HPLC	High performance liquid chromatography
LPMO(s)	Lytic polysaccharide monooxygenase (s)